Research paper

Synthesis, molecular modeling, in vivo study and anticancer activity against prostate cancer of (+) (S)-naproxen derivatives

Kaan Birgül [a, b], Yeliz Yıldırım [c, d], H. Yeşim Karasulu [c, e, **], Ercüment Karasulu [c, f], Abdullah Ibrahim Uba [g], Kemal Yelekçi [g], Hatice Bekçi [h], Ahmet Cumaoğlu [h], Levent Kabasakal [i], Özgür Yılmaz [j], Ş. Güniz Küçükgüzel [a, *]

[a] Department of Pharmaceutical Chemistry, Faculty of Pharmacy, Marmara University, 34854, İstanbul, Turkey
[b] Department of Pharmaceutical Chemistry, Faculty of Pharmacy, Altınbaş University, 34147, Istanbul, Turkey
[c] Center for Drug R&D and Pharmacokinetic Applications (ARGEFAR), Ege University, 35040, İzmir, Turkey
[d] Department of Chemistry, Faculty of Science, Ege University, 35040, Izmir, Turkey
[e] Department of Pharmaceutical Technology, Faculty of Pharmacy, Ege University, 35040, İzmir, Turkey
[f] Department of Biopharmaceutics and Pharmacokinetics, Faculty of Pharmacy, Ege University, 35040, İzmir, Turkey
[g] Department of Bioinformatics and Genetics, Faculty of Engineering and Natural Sciences, Kadir Has University, 34083, İstanbul, Turkey
[h] Department of Pharmaceutical Biochemistry, Faculty of Pharmacy, Erciyes University, 38039, Kayseri, Turkey
[i] Department of Pharmacology, Faculty of Pharmacy, Marmara University, 34660, İstanbul, Turkey
[j] TUBITAK Marmara Research Center, Materials Institute, 41470, Kocaeli, Turkey

ARTICLE INFO

ABSTRACT

In this study, (S)-naproxen thiosemicarbazides (**3a-d**), 1,2,4-triazoles (**4a-c**), triazole-thioether hybride compounds (**5a-p**) were synthesized and their structures (**3a, 3d, 4a** and **5a-p**) were confirmed by FT-IR, ^{1}H NMR, ^{13}C NMR, HR-Mass spectra and elemental analysis. These compounds are designed to inhibit methionine amino peptidase-2 (MetAP2) enzyme in prostate cancer. These compounds (**3d, 5a-p**) evaluated against androgen-independent prostate adenocarcinoma (PC-3, DU-145) and androgen-dependent prostate adenocarcinoma (LNCaP) cell lines by using MTS method. Compounds **5a, 5b, 5d** and **5e** showed 14.2, 5.8, 10.8 and 8.4 μM anticancer activity against PC-3 cell lines, compounds **5e, 5g** and **5n** presented anticancer activity against DU-145 cell lines 18.8, 12.25 and 10.2 μM, and compounds **5g, 5m** and **5n** exhibited anticancer activity against LNCaP cell lines 12.25, 22.76 and 2.21 μM, respectively. Consequently, of these results, compounds **5e** and **5n** showed the highest activities against androgen dependent and independent prostate cancer cell lines, so these compounds could be potent small molecules against prostate cancer. Furthermore, mitogen-activated protein kinase (MAPK) pathway activation, AKT (protein kinase B) phosphorylation and androgen receptor activation of compound **5n** (**SGK636**) were investigated in LNCaP cells by using Western blot method. Compound **5n** (**SGK636**) was also tested against mRNA expression analysis of the Bax, Bcl-2, Caspase 3, Caspase 9 by using real-time PCR analysis. Compound **5n** was given to nude male mice with cancer in comparison to the control group. Compound **5n** was found to reverse the malignant phenotype in the nude male mice, whereas the prostate cancer progressed in the control group. Analysis of some blood parameters in the study showed that they were within the normal values with respect to the control. The blood values of the animals treated according to the control group also exhibited compliance with the blood limit values. Molecular docking and dynamics simulation of compound **5n** binding to Methionine Aminopeptidase 2 (MetAP2) enzyme rationalized its potential activity. In addition, inhibition assay MetAP2 enzyme of compound **5n** was evaluated. Taken together, we suggest compound **5n** to be a potential candidate for prostate cancer therapy.

* Corresponding author. Marmara University, Faculty of Pharmacy, Department of Pharmaceutical Chemistry, Başıbüyük, 34854, İstanbul, Turkey.
** Corresponding author. Ege University, Faculty of Pharmacy, Department of Pharmaceutical Technology, 35040, İzmir, Turkey. Tel.: +90 232 388 22 41.
E-mail addresses: yesim.karasulu@ege.edu.tr (H.Y. Karasulu), gkucukguzel@marmara.edu.tr (Ş.G. Küçükgüzel).

1. Introduction

Cancer, defined as the uncontrolled proliferation and spread of abnormal cells, is one of the most important health problems of today. It is also a public health problem due to its frequent

occurrence and high lethality. The rapid increase in the number of cancer cases in the world, suggests the need to develop new drugs and treatment methods. In recent years directing to an important macromolecular target for drugs has gained importance in novel drug design especially in cancer therapy.

Prostate cancer (PCa) is the second deadliest cancer type after lung cancer in men. After the cancer develops in the prostate, these cancerous cells can spread to the lungs and bones via angiogenesis. Angiogenesis is growth of blood vessels from the existing vasculature. Angiogenesis is crucial development for many diseases such as cancer. The Methionine aminopeptidase-2 (MetAP2) enzyme plays an important role in cell proliferation and cell growth [1]. MetAP2 has been reported as important macromolecular target in prostate cancer ([2−4]) and other cancers [5−9]. Also, many studies revealed that inhibitors of MetAP2 enzyme block angiogenesis and suppress tumor growth. Using the Western blot method, the researchers measured the expression level of MetAP2 in primary benign human prostate epithelial cells (BS403) and prostate tumor cell lines PC3 and DU145, and detected positive staining for MetAP2 in all cancer samples. They stated that MetAP2 detection probes can provide a highly sensitive and non-invasive PET imaging approach for prostate cancer detection, which can be useful in prostate cancer detection, staging and monitoring of therapeutic response [10].

Liu and co-workers reported that triazole and triazole-thioether are MetAP2 inhibitor. In addition, these reachers also reported that the 2-hydroxy-N'-((2S,3R)-3-amino-2-hydroxy-5-(isopropylthio) pentanoyl)-3-chlorobenzohydrazide (A357300) compound, which is from the 2-hydroxy-3-aminoamide class, is also a selective, potent inhibitor of MetAP2 [11]. TNP-470, an irreversible MetAP-2 inhibitor, Logothetis et al. It has been used by patients with advanced androgen-independent prostate cancer and has been found to be biologically active [12].

Although there are no microbiological agents that have been clearly shown to cause prostate cancer development to date, there are scientific data suggesting that the inflammatory process has an important role in prostatic carcinogenesis. In studies on the role of cytokines, which are part of the inflammatory process in prostate cancer, many data were obtained about interleukin-6 (IL-6). Some of the molecular data supporting the role of inflammation in the development of prostate cancer belongs to the COX-2 enzyme, one of the most important mediators of inflammation. In recent years researches also have revealed that COX-2 overexpression is associated with cancer progression. COX-2 overexpression has been shown to increase Bcl-2 expression and reduce apoptosis. As a natural extension of this information, it has been suggested that drugs that inhibit prostaglandin synthesis with COX-2 inhibition should have anti-cancer effects. Epidemiological studies have shown that people who regularly use aspirin or other non-steroidal anti-inflammatory drugs (NSAIDs) reduce the risk of developing some cancers [13].

Naproxen ((+) (S)-2-(6-methoxynapthalene-2-yl)propanoic acid), one of the strongest non-steroidal anti-inflammatory drugs (NSAIDs), inhibits the cyclooxygenase (COX) enzymes both COX-1 and COX-2. Inhibits both COX-1 and COX-2 which are the enzymes of cyclooxygenase (COX). Naproxen displays analgesic, anti-inflammatory, and antipyretic activity. In addition, the researchers reported anticancer and antimicrobial activities of Naproxen derivatives [14].

In cure of advancing prostate cancer, naproxen was discovered to be reliable and effective with early repetitive disease in a phase II clinical trial [15]. In men, with early repetitive disease, naproxen and calcitriol are efficient in safely adjourning the progression and growth of PCa. Directed several weeks after the tumor-initiating agent, naproxen was noticed to be effective in protection of bladder

cancer proliferation [16]. In rodents, naproxen has been shown to be effective as well as other NSAIDs to prevent urinary bladder cancer. By inducing apoptosis and cell cycle arrest toward bladder cancer cells, naproxen displayed anticancer influences. Naproxen inhibited protein kinase B (AKT) phosphorylation and induced apoptosis in rat urinary bladder cancers [17]. In addition, naproxen is inhibitor of IL-6. IL-6 is a pro-inflammatory cytokine that is expressed in prostate tumors [18]. Han and co-workers synthesized a new series of 1,2,4-triazole containing hydrazide-hydrazones that are derived from (S)-Naproxen. Molecular modeling of these compounds studied on human methionine aminopeptidase 2 (MetAP2) and all synthesized compounds were screened for anticancer activity against three prostate cancer cell lines, PC-3, DU-145, LNCaP using the MTS colorimetric method [2,3] (+) (S) -2- {[5-[1- (6-methoxynaphthalen-2-yl) ethyl] -4- (4-fluorophenyl)-4H-1,2,4-triazol-3-yl]sulfanyl}-N'-[(5-nitrofuran-2-yl)methylidene] aceto hydrazide showed the best activity against PC-3 and DU-145 and LNCaP cancer cell lines. The biodistribution of the IRDye800-tag in mice of this compound was evaluated using the IVIS spectrum device. In addition, ex-vivo studies were carried out to determine in which organs this compound accumulates in the urogenital system. Ex-vivo studies have shown that this compound may be promising for the treatment of prostate cancer [3]. Anticancer activity of thiosemicarbazide, triazole and thioether derivatives were determined by researchers [9,19−23].

In this study, thiosemicarbazides (3a-d), 1,2,4-triazoles (4a-c), triazole-thioether hybride molecules of (S)-naproxen (5a-p) were synthesized and also their structures were confirmed by FT-IR, ^{1}H NMR, ^{13}C NMR, HR-Mass spectra and elemental analysis. These compounds (3a, 5a-p) evaluated on the prostate cancer cell lines androgen-independent prostate carcinoma cells (PC-3, DU-145) and androgen-dependent prostate carcinoma cell (LNCaP). Compound 5n was evaluated for apoptotic caspases protein expression in LNCaP cell by using Western blot analysis and Bax, Caspase 9, Caspase 3 and anti-apoptotic BcL-2 mRNA levels. Molecular modeling studies of compound 5n were also performed against MetAP2 active site using molecular modeling tools and inhibition assay of MetAP2 enzyme of compound 5n was evaluated. In addition, in vivo anticancer study of compound 5n was performed in nude mice with LNCaP prostate cancer. In vivo analyses were also carried out in nude mice.

2. Chemistry

To verify the information that naproxen, the starting material of the synthesis in this study, is in the form of S-enantiomer [24], Naproxen compound was tested by using Rudolph Autopol V Plus brand/model polarimeter device according to European Pharmacopoeia (EP) monograph [25]. As reported in EP 7.0, the optical rotation angle of (S)-Naproxen is indicated as 59−62°. 0.5 g Naproxen was dissolved in 25 ml pure ethanol and according to polarization result (+59.246°). Naproxen compound that used in the synthesis is in the S-form.

Naproxen ((S)-2-(6-methoxynapthalene-2-yl)propanoic acid), was refluxed in the methanolic medium with concentrated sulfuric acid as catalyst to obtain methyl ester of naproxen (methyl (S)-2-(6-methoxynaphthalene-2-yl)propanoate) (1) (**CAS Number: 26159−35−3**). Ethanolic medium of naproxen methyl ester and hydrazine hydrate were refluxed to obtain Naproxen hydrazide ((S)-2-(6-methoxynaphthalene-2-yl)propanehydrazide) (2) (**CAS Number: 57475−91−9**). Compound 2 and equimolar substituted isothiocyanates were heated in n-butanol medium to get (S)-2-(2-(6-methoxynaphthalene-2-yl)propanoyl)-N-substitutedphenyl-1-carbothioamide (3a-d). Compound 3a-d was reacted with 4 N NaOH solution to give the 5-(1-(6-methoxynaphthalene-2-yl)

ethyl)-4-(substitutedphenyl)-4H-1,2,4-triazole-3-thiols (**4a-c**). The reaction was monitored by using thin layer chromatography and then neutralized with concentrated hydrochloric acid after its completion. In the last step of the synthesis, the novel thioether compounds, 4-(substitutedphenyl)-5-(1-(6-methoxynaphtalene-2-yl)ethyl)-3-((substitutedbenzyl)thio)-4H-1,2,4-triazoles (**5a-p**) were obtained by the reaction of (S)-Naproxen triazoles (**4a-c**) refluxed in ethanol with substituted benzyl chloride in the presence of K_2CO_3. The general synthesis of the novel (S)-Naproxen derivatives is shown in Scheme 1.

These compounds; **3a, 3d, 4a** and **5a-p** are original compounds synthesized in this study. The structures of all compounds were confirmed by FT-IR and ^{1}H NMR spectroscopic methods and their purities were proven by TLC and elemental analysis. All of reactions were monitored by TLC in different mobile phases, M_1: petroleum ether/dichlorometane/ethylacetate (25:50:25 v/v/v) and M_2: petroleum ether/ethylacetate (60:40, v/v) at 25 °C.

FT-IR analysis of novel thiosemicarbazides, N-(3-chlorophenyl)-2-[2-(6-methoxynaphthalen-2-yl)propanoyl]hydrazinecarbothioamide (**3a**) and N-(4-(trifluoromethyl)phenyl)-2-[2-(6-methoxynaphthalen-2-yl)propanoyl] hydrazinecarbo thioamide (**3d**), showed N−H stretching band at 3299 and 3284 cm^{-1}. The C=O and C=S stretching bands observed at 1673, 1689 cm^{-1} and 1263, 1264 cm^{-1}, of each molecule, respectively. This C=S stretching band demonstrated specific thiosemicarbazide band. The ^{1}H NMR spectra proven the chemical shifts of N_1 protons; 10.18, 10.20, N_2 protons; 9.78, 9.87, and N_4 protons 9.61 and 9.73 ppm with 1H intensity of each molecule, respectively.

Compound **4a**; (S)-5-[1-(6-methoxynapthalen-2-yl)ethyl]-4-(3-chlorophenyl)-4H-1,2,4-triazole-3-thiol was formed as a result of cyclization of Compound **3a**, in ethanolic 4 N NaOH medium. In the FT-IR spectrum of compound **4a**, existence of S−H stretching band at 2775 cm^{-1} without N−H and C=O stretching bands, indicates that compound **4a** may contain the structure of 1,2,4-triazole-3-thione. As stated in the literature, 1,2,4-triazole-3-thione structure could show tautomerism as 1,2,4-triazole-3-thiole structure. The ^{1}H NMR spectra proved the formation of tautomer for this molecule as chemical shift of N−H proton at 13.95 ppm as a singlet. The 1,2,4-triazole compounds (**4b-c**) are also prepared according to the method reported in the literature [26].

The novel thioether compounds (**5a−p**) were obtained from related 1,2,4-triazole with substituted benzyl chloride and potassium carbonate in ethanolic medium. FT-IR studies of these compounds did not show any N−H or S−H stretching bands which could be observed for 1,2,4-triazole molecules. Additionally, ^{1}H NMR studies proved the structure of S−CH$_2$ protons at approximately 4.00 ppm in thioether molecules. S−CH$_2$ protons of some compounds were observed together with CH−CH$_3$ protons as multiplet peaks. In thioether compounds, S−CH$_2$ observed as singlet or double doublet with 2H intensity and their coupling constants observed as 12.9 Hz.

FT-IR spectrum of compound **5n** did not show any N−H or S−H stretching bands which could be seen in 1,2,4-triazole molecules. In this study, ^{1}H NMR proved the specific S−CH$_2$ protons observed together with CH−CH$_3$ protons as multiplet, at nearly 4.00 ppm. Besides this information, three Ar-CH$_3$ protons which found in the molecular structure of compound **5n**, were observed as 9H, singlet around 2.08 ppm. NH or SH protons from the 1,2,4-triazole structure were not observed in ^{1}H NMR spectral data of compound **5n**. The ^{13}C NMR spectra of these compounds verified the proposed
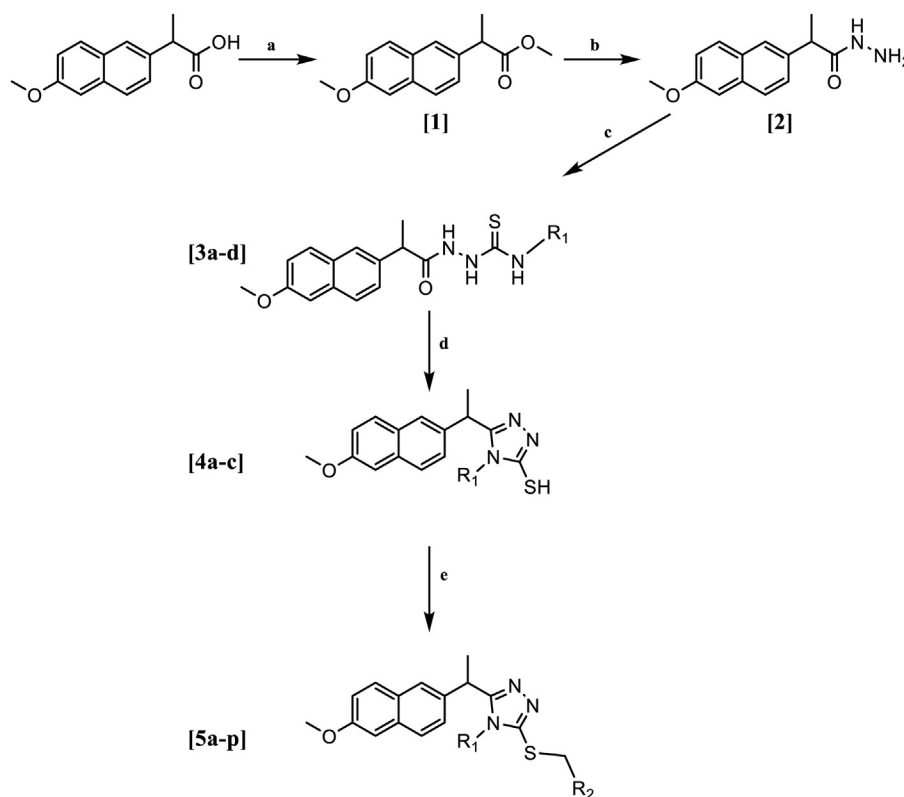
Scheme 1. Reagents and Conditions: (a) CH$_3$OH/H$_2$SO$_4$; (b) NH$_2$NH$_2$· EtOH, (c) substituted phenyl isothiocyanates, n-butanol, EtOH; (d) NaOH (4 N), HCl; (e) substituted benzyl chloride/EtOH/K$_2$CO$_3$.
R$_1$ = 3-chlorophenyl, 4-chlorophenyl, 4-fluorophenyl, 4-(trifluoromethyl)phenyl R$_2$ = phenyl, 4-chlorophenyl, 4-fluorophenyl, 4-methylphenyl, 3-methoxyphenyl, 4-methoxyphenyl, 2,6-dichlorophenyl, 2,4,6-trimethylphenyl.

thioether structure. The peaks resonated at between 34 and 38 ppm $S-\underline{C}H_2$ protons in the ^{13}C NMR spectra of thiothers.

High-resolution mass spectrometry (HR-MS) is an impressive tool with high resolution and high mass accuracy properties, it is used in the analysis of the compounds, determinate of the content elements and verify the empirical formula and molecular weight of compound and its fragments, under 5 mmu proclivity between the calculated and experimental *m/z* value of compound and fragment ions. For compound 5n, the ionization method was electron spray impact (ESI) and when mass spectrum was examined, compound **5n** molecular ion peak catch Na+ from medium due to application of ESI method.

3. Molecular modeling studies

Angiogenesis is the growth of blood vessels from the existing vasculature. Angiogenesis is crucial for the progression of some diseases such as cancer. The MetAP2 enzyme is a target for potent antiangiogenesis due to of its role in cell proliferation and cell growth. The binding mode of all the synthesized novel compounds against MetAP2 was predicted and the resulting binding energy and inhibitor constant (Ki) were estimated (Table 1). All the compounds bound to the active site of MetAP2 (some in opposite orientation (Fig. 1(A)) and showed potential inhibition of MetAP2. Although Compound 5n was found to have lower binding affinity than most compounds under study, it showed good binding mode with relatively less steric clashes. In addition, 100 ns-MD simulations were carried out on both the unbound MetAP2 and MetAP2-Compound **5n** complex to further relax the complex and to examine the stability of Compound **5n** binding mode. MD simulation has been successfully applied to study the stability of small molecules bound to MetAP2 [27].

The root-mean-square deviation (RMSD) profiles revealed that MetAP2-Compound **5n** demonstrated higher stability compared with the unbound form (Fig. 1(B)). Examination of a representative structure for the most abundant cluster showed that the binding pose of compound 5n was significantly refined (Fig. 1(C)). Compound **5n** formed a H-bond interaction with Ser224 via methoxy group and with Asn329 via fluoro substituent attached to the para position of the 1st phenyl group. The same fluoro group formed a halogen interaction with Glu364. Two π-π interactions with His231, and 2 π-alkyl interactions deep inside the tunnel. Other important interaction includes hydrophobic interactions near the

entrance, a π-sigma interaction with Phe219, and a π-π T-shaped interaction with Tyr444 (Fig. 1(D)).

4. Biological activity of synthesized compounds 3d, 5a-p

4.1. In vitro anticancer activity of 3d, 5a-p

In this study, (+) (S) Naproxen thiosemicarbazides, triazoles and thioethers were synthesized and evaluated for anticancer activity. Compounds **3d**, **5a-p** were evaluated in vitro for their anticancer activity against three human prostate cancer cell lines: PC-3, DU-145 (androgen-independent human prostate adenocarcinoma) and LNCaP (androgen-sensitive human prostate adenocarcinoma) cancer cell lines. The cytotoxic evaluation was made in MTS assay; and subsequently IC_{50} values have been obtained. Cisplatin is a non-specific antineoplastic drug used in the treatment of various tumors. It has revolutionized the treatment of urogenital system cancer such as testicular cancer, bladder cancer, kidney and ureter tumors, prostate cancer and ovarian cancer, and has gained the potential to cure a previously fatal disease. Therefore, cisplatin was chosen as a positive control drug. IC_{50} results of synthesized compounds are noticed in Table 2.

Compound **5n** demonstrated anticancer activity against the PC-3, DU-145 and LNCaP prostate cancer cell lines with IC_{50} values of 43.3, 10.2 and 2.21 μM, respectively.

According these results, compounds **5a**, **5b**, **5d**, **5e**, **5n** and **5p** showed anticancer activity against PC-3 with IC_{50} values in the range of 5,8−43,3 μM. Against DU-145 cell line; compounds **5g**, **5l** and **5n** were found anticancer activity nearly as cisplatin as which was used as a positive control in our study, 12.25, 19.2 and 10.2 μM, respectively. When the anticancer activity was examined against LNCaP cancer cells, IC_{50} values of compounds **5g**, **5m** and **5n** were found to have 12.25, 14.45 and 2.21 μM activity, respectively. With all these results, compound **5n**, was chosen as the leading compound for further studies.

Compound **5n**, showed significant anticancer activity against all androgen-dependent and androgen-independent prostate cancer cell lines, PC-3, DU-145 and LNCaP with 43.3, 10.2 and 2.21 μM, respectively. Anticancer activity of novel (+) (S)-naproxen 1,2,4-triazole-thioether hybrid structures, are different from each other due to different R_1 and R_2 substituents. Compare between R_1 substituents, 4-fluorophenyl group shows better activity than 4-chlorophenyl groups nearly in all cell lines. When we compare R_2

Table 1
Molecular docking results of synthesized compounds.

Lab Code	Compound	R_1	R_2	Binding Energy ΔG (kcal/mol)	Inhibition constant, Ki (nanoM)
SGK-624	**3a**	$-C_6H_4-Cl$ (3)	−	−11.03	8.27
SGK-606	**3d**	$-C_6H_4-CF_3-$(4)	−	−8.37	731.62
SGK-625	**4a**	$-C_6H_4-Cl$ (3)	−	−9.1	212.47
SGK-607	**5a**	$-C_6H_4-Cl$ (4)	$-C_6H_5$	−10.63	16.2
SGK-608	**5b**	$-C_6H_4-Cl$ (4)	$-C_6H_4-Cl$ (4)	−11.02	8.29
SGK-609	**5c**	$-C_6H_4-Cl$ (4)	$-C_6H_3-Cl_2$ (2,6)	−9.55	62.87
SGK-610	**5d**	$-C_6H_4-Cl$ (4)	$-C_6H_4-F$ (4)	−11.29	5.3
SGK-611	**5e**	$-C_6H_4-Cl$ (4)	$-C_6H_4-CH_3$ (4)	−10.56	18.06
SGK-613	**5f**	$-C_6H_4-F$ (4)	$-C_6H_4-Cl$ (4)	−11.17	6.49
SGK-614	**5g**	$-C_6H_4-F$ (4)	$-C_6H_3-Cl_2$ (2,6)	−10.79	12.38
SGK-615	**5h**	$-C_6H_4-F$ (4)	$-C_6H_4-F$ (4)	−9.98	48.27
SGK-616	**5i**	$-C_6H_4-F$ (4)	$-C_6H_4-CH_3$ (4)	−9.97	49.17
SGK-622	**5j**	$-C_6H_4-Cl$ (4)	$-C_6H_4-OCH_3$ (3)	−9.97	49.43
SGK-623	**5k**	$-C_6H_4-Cl$ (4)	$-C_6H_4-OCH_3$ (4)	−9.63	87.82
SGK-634	**5l**	$-C_6H_4-F$ (4)	$-C_6H_4-OCH_3$ (3)	−11.17	6.47
SGK-635	**5m**	$-C_6H_4-F$ (4)	$-C_6H_4-OCH_3$ (4)	−11.03	8.18
SGK-636	**5n**	$-C_6H_4-F$ (4)	$-C_6H_2-(CH_3)_3$ (2,4,6)	−9.17	191.06
SGK-639	**5o**	$-C_6H_4-Cl$ (3)	$-C_6H_3-Cl_2$ (2,6)	−9.57	96.72
SGK-642	**5p**	$-C_6H_4-Cl$ (3)	$-C_6H_2-(CH_3)_3$ (2,4,6)	−11.03	8.16

Fig. 1. Docking poses of the study compounds: the compounds bound to MetAP2 active site with different mode **(A)**. Root-mean-square deviation (RMSD) of unbound MetAP2 (blue) and MetAP2-Compound **5n** complex (Red) **(B)**. Binding mode Compound **5n** in the representative structure of MetAP2-Compound **5n** complex derived from molecular dynamics simulation **(C)**, and the resulting interaction diagram between compound **5n** and the amino acid residues in the catalytic channel of MetAP2 enzyme **(D)**. (For interpretation of the references to color in this figure legend, the reader is referred to the Web version of this article.)

substituents, not only 4-methoxyphenyl group, but also 4-chlorophenyl groups shows bad activity against DU-145 and LNCaP cell lines. But when 2,4,6-trimethylphenyl group was added instead of 4-methoxyphenyl and 4-chlorophenyl groups, increased anticancer effect observed. Additionally, when the substituents on both sides replaced with a substituent which including at least one electronegative atom, the activity decreases. Despite of all these information showed that thiosemicarbazides and 1,2,4-triazoles-thioether hybride compounds may play major role in treatment of prostate cancer.

4.2. Western blot studies of compound 5n

In vitro, the activation (phosphorylation) and the signal transduction mechanisms of the compounds that are effectively detected in LNCaP cells containing the androgen receptor in the prostate cancer cells and the apoptosis in the prostate cancer cells were studied. In this context, substances that are as effective as cell

Table 2
IC_{50} results (μM) of novel (+) (S)-naproxen derivatives against PC-3, DU-145 and LNCaP cell lines.

Lab Code	Compound	R_1	R_2	PC-3	DU-145	LNCaP
	Cisplatin			39.9	9.6	20.7
SGK-624	**3a**	$-C_6H_4$-Cl (3)	−	NT	NT	NT
SGK-606	**3d**	$-C_6H_4$-CF_3-(4)	−	64.3	62.2	92.8
SGK-625	**4a**	$-C_6H_4$-Cl (3)	−	NT	NT	NT
SGK-607	**5a**	$-C_6H_4$-Cl (4)	$-C_6H_5$	14.2	35.8	50.4
SGK-608	**5b**	$-C_6H_4$-Cl (4)	$-C_6H_4$-Cl (4)	5.8	109.1	109.9
SGK-609	**5c**	$-C_6H_4$-Cl (4)	$-C_6H_3$-Cl_2 (2,6)	34.7	36.1	>400
SGK-610	**5d**	$-C_6H_4$-Cl (4)	$-C_6H_4$-F (4)	10.8	33.6	33.9
SGK-611	**5e**	$-C_6H_4$-Cl (4)	$-C_6H_4$-CH_3 (4)	8.4	18.8	52.2
SGK-613	**5f**	$-C_6H_4$-F (4)	$-C_6H_4$-Cl (4)	400 ≤ IC_{50}	57.35	400 ≤ IC_{50}
SGK-614	**5g**	$-C_6H_4$-F (4)	$-C_6H_3$-Cl_2 (2,6)	215.7	12.25	12.25
SGK-615	**5h**	$-C_6H_4$-F (4)	$-C_6H_4$-F (4)	400 ≤ IC_{50}	60.2	104.3
SGK-616	**5i**	$-C_6H_4$-F (4)	$-C_6H_4$-CH_3 (4)	229.0	44.3	400 ≤ IC_{50}
SGK-622	**5j**	$-C_6H_4$-Cl (4)	$-C_6H_4$-OCH_3 (3)	138.2	400 ≤ IC_{50}	162.0
SGK-623	**5k**	$-C_6H_4$-Cl (4)	$-C_6H_4$-OCH_3 (4)	400 ≤ IC_{50}	72.6	400 ≤ IC_{50}
SGK-634	**5l**	$-C_6H_4$-F (4)	$-C_6H_4$-OCH_3 (3)	211.1	19.2	14.45
SGK-635	**5m**	$-C_6H_4$-F (4)	$-C_6H_4$-OCH_3 (4)	400 ≤ IC_{50}	400 ≤ IC_{50}	22.76
SGK-636	**5n**	$-C_6H_4$-F (4)	$-C_6H_2$-$(CH_3)_3$ (2,4,6)	43.3	10.2	2.21
SGK-639	**5o**	$-C_6H_4$-Cl (3)	$-C_6H_3$-Cl_2 (2,6)	165.2	400 ≤ IC_{50}	73.7
SGK-642	**5p**	$-C_6H_4$-Cl (3)	$-C_6H_2$-$(CH_3)_3$ (2,4,6)	16.3	93.3	400 ≤ IC_{50}

(NT: Not Tested)

reference (cisplatin) are selected and the mechanism of how these substances affect cell viability is examined. It was also included in the study as a partial positive control to test randomly selected compound effects that did not affect cell viability. In this context, androgen receptor activation in LNCaP cells and its affected (MAPK) mitogen-activated protein kinase pathway activation and AKT (protein kinase B) phosphorylation were investigated (Fig. 2).

In this study, IC$_{50}$ dose of compound 5n was determined as 2.21 μM. LNCaP cells were exposed to compound 5n for 15, 60 and 120 min at concentrations 5 and 20 μM. The compounds significantly reduced androgen receptor phosphorylation. Also the compound significantly reduced phosphorylation of AKT, ERK/MAPK, P38/MAPK and JNK/MAPK (Fig. 3). Compound 5 m (SGK 635) was used as a positive control as no inhibition was seen for at least two cell lines. The Western blot study of the positive control compound 5 m and compound 5n is given in Fig. 3.

4.3. Apoptosis results of SGK 636

After LNCaP cells were exposed to compound 5n (5 and 20 μM) for 3 and 6 h, we performed mRNA expression analysis of the Bax, Bcl-2, Caspase 3, Caspase 9. Real-time PCR analysis confirmed that there was a time-dependent rise in the expression levels of pro-apoptotic Bax, Caspase 3 and Caspase 9 in the compound 5n-treated LNCaP cells compared with the control. In addition to these results, anti-apoptotic Bcl-2 mRNA levels were significantly decreased in compound 5n-treated LNCaP. All these results showed that treatment with compound 5n caused an important rise in apoptotic markers and decreased in anti-apoptotic markers (Fig. 4).

4.4. Methionine Aminopeptidase-2 assay

Compound 5n was tested in vitro for inhibitory activity towards MetAP2 in a spectrophotometric inhibition assay. As shown in Fig. 5, Compound 5n could inhibit the enzymatic action up to 42−77.7% within the studied dosage (12.50−200.00 μM). The inhibition efficiency was enhanced by increasing the concentration of compound 5n.

Fig. 3. AR/AKT and AR/MAPK pathway inhibition in compound 5n (SGK 636) treated cells (SGK 635 (compound 5m) was used as positive control).

5. In vivo studies

5.1. Development of prostate cancer in nude male mice

The inhibition of Compound 5n in androgen dependent LNCaP

Fig. 2. Compound 5n (SGK 636) inhibited non genomic androgen receptor signaling pathway by suppressed the phosphorylation of P38/MAPK, ERK/MAPK, AKT and AKT mediated AR transactivation.
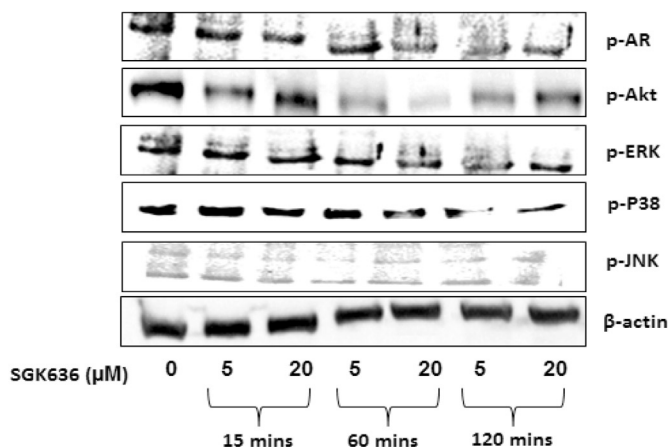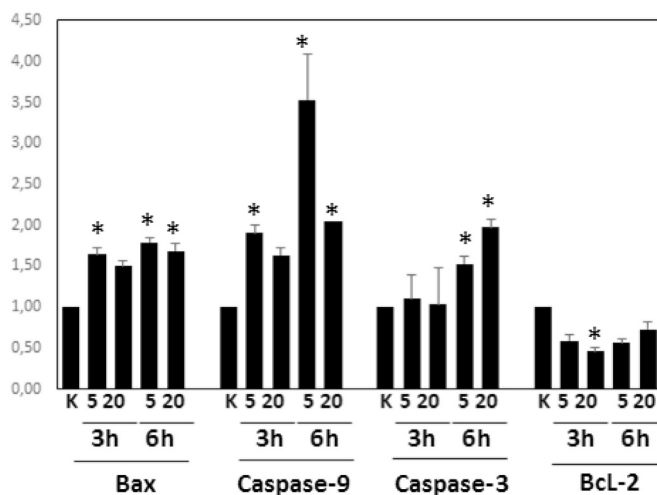

Fig. 4. Compound 5n induced apoptotic genes including Bax, Caspase 9, Caspase 3 and supressed anti-apoptotic BcL-2 mRNA levels in LNCaP cell. N = 3, *p < 0,05 control K: control.
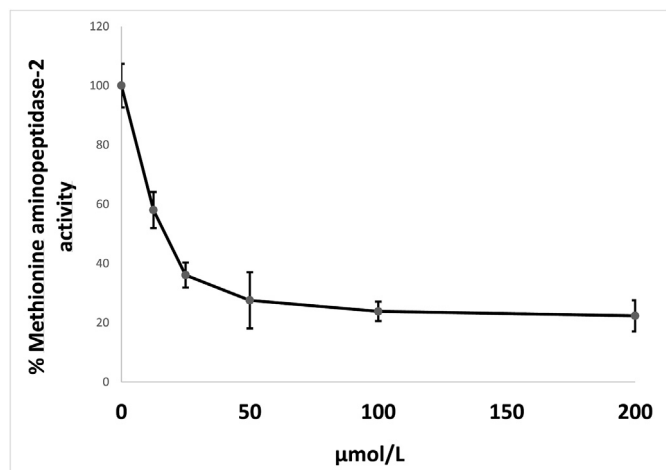
Fig. 5. In vitro inhibitory activity towards MetAP2 assay of Compound **5n**.

prostate cancer cell with a value of 2.2 μM in vitro study, being effective on phosphorylation mechanism and increasing apoptosis led us to study in prostate cancer in vivo. Nude male mouse and IVIS spectrum device were used for this study.

Tumor size and development in cancer animal models generated using LNCaP cells were monitored using the IVIS spectrum instrument and the Rediject 2DG-750 Probe. Glucose is used in imaging of cancerous tissues due to higher accumulation in cancerous tissues compared to other cells (Fig. 6).

5.2. Results of compound **5n** in nude male mice with prostate cancer

The prostate cancer nude mice were treated with compound **5n** for 15 days in order to examine the prostate cancer treatment potential of the compound **5n** active substance. The obtained IVIS images results of 0.27 mg compound **5n**/100 μL serum physiological and no treatment groups are shown in Figs. 7 and 8.

When the IVIS images are examined in Figs. 7 and 8, the ROI value of cancerous tissue treatment with compound **5n** in 15 days decreased between 55 and 70%, whereas tumor activity increased 5-fold in the untreated group.

5.3. Blood analysis of treated prostate cancer animals

The results of blood parameters such as Albumin (ALB), Alkaline Phosphatase (ALP), Alanine Transaminase (ALT), Total Bilirubin (TBIL), Blood Urea Nitrogen (BUN), Phosphate (PHOS), Keratin (CRE), Glucose (GLU), Sodium (Na), Potassium (K), Total Protein (TP), and globulin (GLOB) of healthy mice and prostate cancer nude mice with compound **5n** treated and untreated were shown in Table 3.

ALP and ALT values of cancer nude mice compared to healthy animals were significantly increased. The results of 3 doses compound 5n treatment group is much closer to that of healthy nude mice. ALP is an enzyme that is present in various organs such as kidney, bone and liver and enables various chemical reactions to take place. Increased ALP values are considered as precursors of various bone, liver, heart and cancer diseases [28−30]. The decrease in ALP and ALT levels after treatment with cancer nude mice is consistent with the aim of our study.

When BUN and CRE values are examined, it is seen that cancer and healthy nude mice have very close values. Urea is a metabolite in the human body that contains nitrogen as a result of protein destruction in the liver and more than 90% is excreted via the kidney. BUN test results are not in the desired range indicates that the kidney or liver is not working properly. Clinicians generally use Blood Urea Nitrogen (BUN)/Creatine (CRE) ratio [31,32]. According to the obtained results as the BUN/CRE ratio, the healthy, compound 5n no treatment and compound 5n treatment groups were 137, 135, and 86, respectively. The decrease in the ratio of the treated group compared to healthy and untreated cancer groups may be interpreted as the decrease in urea formation seen in liver patients.

The glucose values obtained from the blood results of our experimental groups are compared, an increase is observed in cancer animals. It is recorded in the literature that an increase in glucose levels in the blood of cancer nude mice is observed [33]. As a result of 3 doses compound 5n treatment group decreased to levels close to healthy mice.

When the Na and K values in the blood of our groups are examined, it is seen that the Na values do not much change while the K value increases in untreated cancer animals by 100% depending on the disease. The K value of the group treated with compound 5n was found to be consistent with the results of healthy mouse.

The values of ALB, TBIL, PHOS, TP and GLOB in our study groups did not significantly change after 3 doses of treatment.
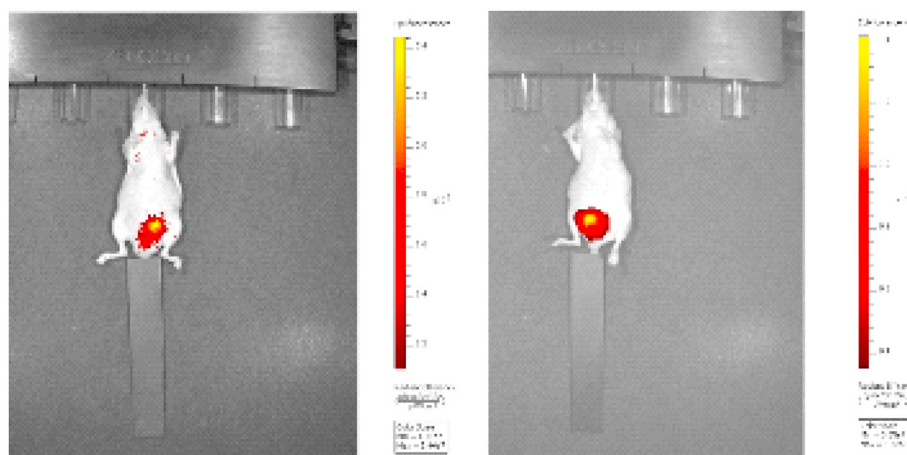

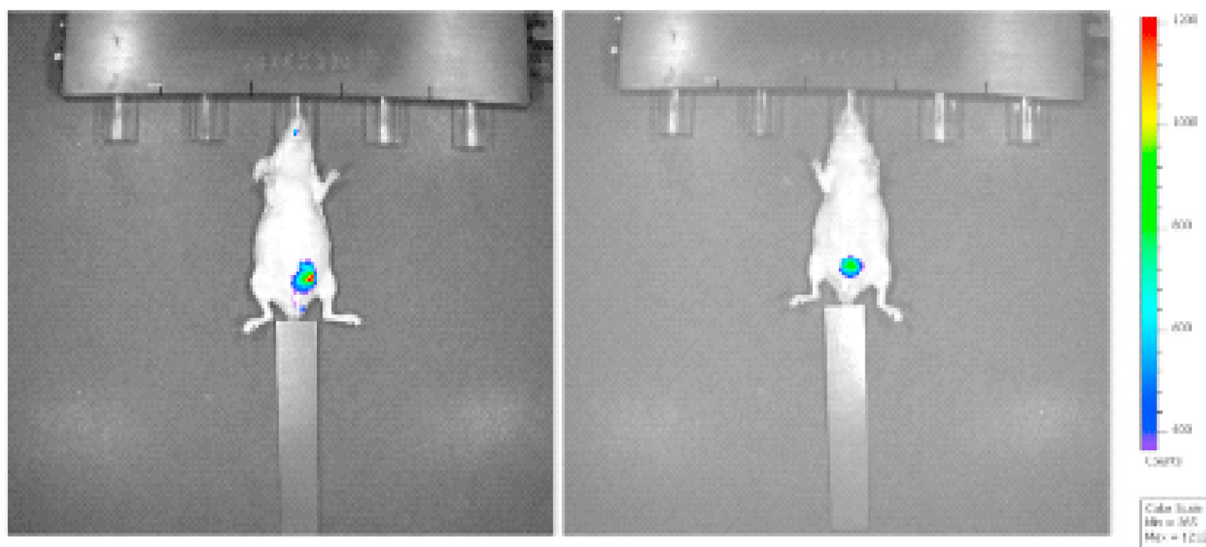**Fig. 6.** IVIS Spectrum Images of Prostate Cancer Nude mice models.

Fig. 7. IVIS images of nude mice treated with compound **5n**.
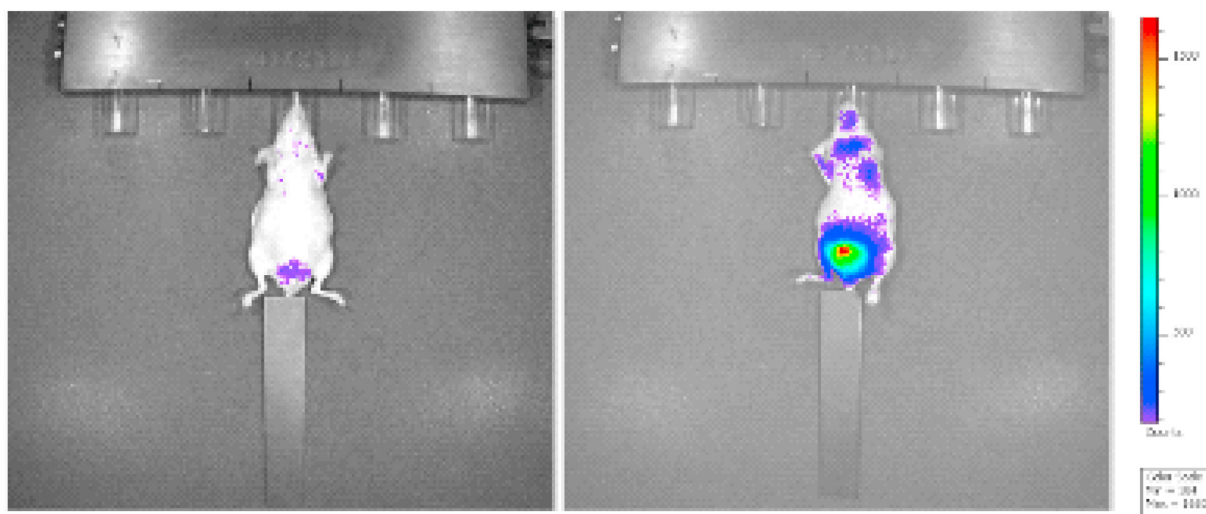

Fig. 8. IVIS images of nude mice not treated with compound **5n**.

Table 3
The blood results of healthy mice and prostate cancer nude mice with compound **5n** treated and untreated.

	Compound 5n no treatment group	Compound 5n treatment group	Healthy group
ALB (G/DL)	2.60 ± 0.36	1.25 ± 0.35	1.90 ± 0.20
ALP (U/L)	144.50 ± 83.50	58.00 ± 20.00	70.50 ± 8.50
ALT (U/L)	679.50 ± 71.50	64.50 ± 20.50	33.00 ± 0.00
TBIL (MG/DL)	0.27 ± 0.05	0.30 ± 0.00	0.20 ± 0.00
BUN (MG/DL)	27.00 ± 2.16	21.50 ± 4.50	27.50 ± 0.00
PHOS (MG/DL)	10.07 ± 1.68	7.15 ± 0.35	8.10 ± 1.10
CRE (MG/DL)	0.2 ± 0.07	0.25 ± 0.05	0.20 ± 0.00
GLU (MG/DL)	192.00 ± 33.00	154.00 ± 28.00	126.00 ± 26.00
Na (MMOL/L)	148.33 ± 1.89	137.50 ± 4.50	142.50 ± 0.05
K (MMOL/L)	10.70 ± 2.20	5.60 ± 0.00	5.80 ± 0.01
TP (G/DL)	5.70 ± 0.40	5.30 ± 0.20	5.20 ± 0.00
GLOB (G/DL)	3.17 ± 0.31	3.60 ± 0.00	3.00 ± 0.00

6. Conclusion

Naproxen (+) (S)-2-(6-methoxynaphthalen-2-yl)propanoic acid, the carboxylic acid derivative containing the naphthalene structure, has been a non-steroidal agent with analgesic, antipyretic, and anti-inflammatory effects. In addition, many studies have shown that naproxen has anticancer effects against many types of cancer. These observations led us synthesize new naproxen

derivatives and evaluate their anticancer activities.

In this study, (S)-Naproxen derivatives were synthesized and the structures of these compounds were proved by FT-IR, ^{1}H NMR, ^{13}C NMR and elemental analysis. N−H or S−H stretching bands could be seen in the FT-IR spectrum of the thioether derivatives whereas the same bands are not observed in the spectrum of the 1,2,4-triazole-thione/thiole structures. Also, because of the added benzyl group to the molecule, S−CH$_2$ protons were observed as singlet or double doublet between 4.17 and 4.38 ppm. Addition of this information, when the ^{13}C NMR spectra of synthesized compounds were examined, the peak of carbon belonging to S−CH$_2$, was observed between 34 and 38 ppm. The anticancer activities of the compounds **3d, 5a-p** were evaluated in vitro by using the MTS colorimetric method against PC-3 and DU-145 (androgen-independent prostate adenocarcinoma) and LNCaP (androgen-dependent prostate adenocarcinoma) cell lines. When the structure activity relationships of the synthesized compounds are studied, the R1 position of the 4 chlorophenyl ring seems to play a significant role in the biological activity. When the phenyl group at R2 positions is substituted with alkyl or electronegative substituents, the activity increases. However, the activity decreases when methoxy group is added to meta or para position of the phenyl ring. The activity differences among the compounds are also observed in 4 fluorophenyl derivatives in R1 side. The addition of electronegative groups in R2 position of the phenyl ring decreases the activity. However, the addition of the methyl group in 2nd, 4th and 6th position of the phenyl ring, increased the activity. Furthermore, the overall evaluation of the compounds shows us that the thioether derivatives shows higher anticancer activity than the thiosemicarbazide compound.

Compound **5n** was found to have anticancer activity in LNCaP cell line at IC$_{50}$ values of 2.21 μM. To support these findings, molecular modeling studies against MetAP2 enzyme were performed. Compound **5n** with the values of $\Delta G = -9.17$ kcal/mol, $Ki = 191.06$ nanoM was found to be the most potent MetAP2 inhibitor among compounds. According to these results, there was a correlation between molecular modeling and anticancer activity results. Therefore, here, we attempted to elucidate the mechanism of action of compound **5n** on LNCaP cell line via MAPK and AKT signaling and apoptosis pathway.

In this study, obtaining promising results at the in vitro anticancer activity studies of the triazole-thioether hybrid compound **5n** on LNCaP prostate cancer cell line led to the in vivo studies. In male nude mice in which prostate cancer was established with LNCaP cancer cells, the compound **5n** stopped cancer development and invasion, also significant results were obtained in blood values in the cancerous animal.

In conclusion, in the light of the findings obtained after in vitro and in vivo studies, compound **5n** is a promising compound for prostate cancer. As a result of preclinical and clinical studies planned in the future, we think that it will be a promising candidate molecule in the treatment of prostate cancer and may be among the other molecules available in the market.

7. Experimental protocols

7.1. Chemistry

7.1.1. Materials and methods

All reagents were bought from Sigma Aldrich, Alfa Aesar or Merck. Synthesized of molecule was performed in Daihan SMHS-3 Hot Plate and Daihan MS-MP8 magnetic stirrer. The reaction monitoring and impurity control of the synthesized compounds were carried out by thin layer chromatography method. In TLC studies 0.2 mm thick silica gel F-254 Merck TLC plates were used as adsorbents. The purity of the compounds was controlled on TLC plates in a solvent system contain mixture of petroleum ether/ ethylacetate (60:40, v/v) and petroleum ether/dichlorometane/ ethylacetate (25:50:25 v/v/v) at 25 °C. The spots of compounds were detected under UV light (254 nm, t: 25 °C). Melting point of the synthesized compounds were detected in Stuart SMP 20 and uncorrected. The optical rotation angle of the naproxen was performed according to European Pharmacopoeia with Rudolph Autopol V Plus. FT-IR spectra were run on PerkinElmer − FT-IR Spectrum BX spectrophotometer. Elemental analysis were carried out on CHNS-932 (LECO). ^{1}H NMR spectra were recorded BRUKER Avance-DPX 300 MHz and Agilent VNMRS 500 MHz. Elemental analysis and ^{1}H NMR appliances are located in Inonu University Scientific and Technological Research Center. ^{13}C NMR spectra were recorded Agilent VNMRS 125 MHz which located in Istanbul Technical University and BRUKER Avance-DPX 75 MHz, which located in Inonu University Scientific and Technological Research Center. HR-MS spectra utilizing ESI ionization techniques were carried out using ICR Apex-Qe instrument Xenolight RediJect 2-DG-750 Probe was purchased from PerkinElmer. Phosphate buffer was obtained from Sigma-Aldrich. All other chemicals were in analytical quantity.

7.2. General procedure for the synthesis of compounds

7.2.1. Preparation of (S)-methyl 2-(methoxynapthalen-2-yl) propanoate (1, CAS Number: 26159-35-3) and (S)-2-(6-methoxy-2-naphthyl)propanoic acid hydrazide (2, CAS Number: 57475-91-9)

(+) (S)-Naproxen (0.01 mol) and methanol (20 ml) were refluxed for 4h in a few drops of concentrated sulfuric acid. The reaction is monitored by TLC and end of the reaction cooled and neutralized with 10% NaHCO$_3$. The solid compound is filtered, dried and recrystallized from methanol. Yield: %85; M. P. 92−94 °C (lit: 88 °C) [26].

Compound **1** (0.01 mol, 30 ml) and hydrazine hydrate (100%, 25 ml) was added and refluxed in ethanolic median for 2h. End of the reaction, the flask was cooled, diluted with water and kept in fridge overnight. The solid were filtered, washed with water and recrystallized with methanol. White solid, yield 82% and M. p. 98−100 °C (lit 94 °C). Each compounds were studied by Amir et al. [26].

7.2.2. Synthesis of (S)−N-(arylsubstitued)-2-[2-(6-methoxynaphthalen-2-yl)propanoyl]hydrazinecarbothioamides (3a-d)

Compound **2** (0.01 mol) and substituted phenyl isothiocyanate (0.011 mol) were refluxed 8 h 50 ml of n-butanol. End of the reaction, butanol were evaporated and washed with cold ethanol. The solid compound filtered, dried and recrystallized with ethanol. Compound **3b**; **CAS Number: 1003001−31−7,** N-(4-chlorophenyl)-2-[2-(6-methoxynaphthalen-2-yl)propanoyl]hydrazinecarbothioamide and compound **3c**; **CAS Number: 2361527−36−6** N-(4-fluorophenyl)-2-[2-(6-methoxynaphthalen-2-yl)propanoyl]hydrazinecarbothioamide were synthesized from Amir et al. [26]. Compounds **3a** and **3d** are original compounds synthesized in this study.

7.2.3. General synthesis of (S)-5-[1-(6-methoxynapthalen-2-yl) ethyl]-4-substituted-4H-1,2,4-triazole-3-thioles (4a-c)

Compounds **3a-c** were refluxed 4h in 4 N NaOH medium. In the end, concentrated HCl were used for neutralizing and obtained solid. The solid compound filtered, dried and recrystallized with ethanol. Compound **4b CAS Number: 1003001−43−1,** 4-(4-chlorophenyl)-5-[1-(6-methoxynaphthalen-2-yl)ethyl]-4H-1,2,4-triazole-3-thiol and compound **4c**; **CAS Number: 1003001−45−3,**

4-(4-fluorophenyl)-5-[1-(6-methoxynaphthalen-2-yl)ethyl]-4H-1,2,4-triazole-3-thiol compounds were synthesized by Amir et al. [26]. Compound **4a** is original compound synthesized in this study.

7.2.4. General synthesis of 4-substitued-5-(1-(6-metoxynaphtalen-2-yl)-3-((substituedbenzyl)thio)-4H-1,2,4-triazoles (*5a-p*)

Compounds **4a-c**, equimolar of substituted benzyl chlorides and potassium carbonate (K_2CO_3) were added in ethanolic median and refluxed 24 h. After cooling down at room temperature, the solvent was evaporated and get solid compound. After than, solid compound was filtered, recrystallized with ethanol.

7.2.4.1. (S)−N-(3-chlorophenyl)-2-(2-(6-methoxynapthalen-2-yl) propanoyl)hydrazine-1-carbothioamide (3a). Yield 83.7%, Mp: 194.7−196 °C, Rf x 100 (M_1):27, white solid. ^{1}H NMR: (300 MHz) (DMSO-d_6/TMS) δ ppm: 1.48−1.50 (d, J = 6.9 Hz, 3H, −CH−C<u>H</u>$_3$); 3.85−3.87 (d, 1H, C<u>H</u>−CH$_3$ and 3H, O−CH$_3$); 7.16−7.80 (m, 10H, Ar−<u>H</u>); 9.61 (s,1H, −NH−N<u>H</u>−C=S−NH-); 9.78 (s, 1H, NH−N<u>H</u>−C= S−NH-); 10.18 (s, 1H, −C=O−N<u>H</u>). FT-IR v$_{max}$ (cm^{-1}): 3337, 3299, (Thiosemicarbazide *N*−H); 1673 (C=O); 1263 (C=S). Anal Calcd for C$_{21}$H$_{20}$ClN$_3$O$_2$S (% calculated/found): C: 60.94/61.77, H: 4.87/5.13, N: 10.15/10.30; M. W: 413.92 g/mol.

7.2.4.2. (S)−N-[4-(trifluoromethyl)phenyl]-2-(2-(6-methoxynapthalen-2-yl)propanoyl) hydrazine-1-carbothioamide (3d). Yield: 67%, Mp: 193.8 °C, Rf x 100 (M_1):30, white solid. ^{1}H NMR: (300 MHz) (DMSO-d_6/TMS) δ ppm: 1.48−1.50 (d, J = 7.2 Hz, 3H, −CH−C<u>H</u>$_3$); 3.83−3.86 (d, 1H, -C<u>H</u>-CH$_3$ and 3H −O−CH$_3$); 7.13−7.80 (m, 10H, Ar−H); 9.73 and 9.87 (s, 1H, −NH−N<u>H</u>-C=S and s, 1H, −C=S−N<u>H</u>); 10.20 (s, 1H, −C=O−N<u>H</u>). FT-IR v$_{max}$ (cm^{-1}): 3284 (Thiosemicarbazide *N*−H), 1689 (C=O), 1264 (C=S), 1029 (C−F). Anal Calcd for C$_{22}$H$_{20}$F$_3$N$_3$O$_2$S (calculated/found) C: 59.05/ 58.70, H: 4.51/4.37, N: 9.39/9.36, S:7.17/7.04; M. W: 447.48 g/mol.

7.2.4.3. (S)-4-(3-chlorophenyl)-5-(1-(6-methoxynaphtalen-2-yl) ethyl)-4H-1,2,4-triazole-3-thione (4a). Yield: 97.3%, Mp: 205.3−207.9 °C, Rf x 100 (M_2): 55, white solid. ^{1}H NMR (300 MHz) (DMSO-d_6/TMS) δ ppm: 1.57−1.58 (d, J = 7.2 Hz, 3H, −CH−C<u>H</u>$_3$); 3.85 (s, 3H, O−CH$_3$); 4.07−4.10 (q, 1H, -C<u>H</u>-CH$_3$); 6.98−7.66 (m, 10H, Ar−<u>H</u>); 13.95 (s, 1H, -N<u>H</u>). FT-IR v$_{max}$ (cm^{-1}): 2775 (Triazole *S*−H), 1632, 1607, 1565, 1487, 1388 (triazole C=N), 818 (Ar−Cl). Anal Calcd for C$_{21}$H$_{18}$ClN$_3$O$_2$S (% calculated/found): C: 63.71/62.83, H: 4.58/ 5.05, N: 10.61/10.01, S: 8.10/7.69; M. W: 395.91 g/mol.

7.2.4.4. (S)-3-(benzylthio)-4-(4-chlorophenyl)-5-(1-(6-methoxynaphtalen-2-yl)ethyl)-4H-1,2,4-triazole (5a). Yield: 20%, Mp: 134−137 °C, Rf x 100 (M_2): 17, white solid. ^{1}H NMR: (300 MHz) (DMSO-d_6/TMS) δ ppm: 1.64 (d, J = 6.9 Hz, 3H, −CH−C<u>H</u>$_3$); 3.85 (s, 3H, O−CH$_3$); 4.10 (q, J = 7.2 Hz, J = 7.2 Hz, 1H, -C<u>H</u>-CH$_3$); 4.28 (s, 2H, S−C<u>H</u>$_2$); 7.00−7.66 (m, 15H, Ar−<u>H</u>). ^{13}C NMR (125 MHz, DMSO-d_6) δ$_C$ ppm; 158.34 (C-6), 157.57 (C-18), 150.29 (C-14), 137.53 (C-33), 137.36 (C-28), 134.82 (C-22), 133.50 (C-9), 132.18 (C-2), 129.81 (C-3), 129.74 (C-1), 129.45 (C-7), 129.32 (C-10), 128.87 (C-25, C-26), 128.68 (C-30, C-29), 127.84 (C-8), 127.47 (C-23, C-24), 126.18 (C-31, C-32), 125.71 (C-27), 119.12 (C-5), 106.16 (C-4), 55.60 (C-12), 37.44 (C-13), 36.88 (C-21), 21.23 (C-19). FT-IR v$_{max}$ (cm^{-1}): 3052, 3034 (*C*−H), 1633 (C=N), 1227 (*C*−S). Anal Calcd for C$_{28}$H$_{24}$ClN$_3$OS 0.1/3H$_2$O (calculated/found) C: 69.19/68.35, H: 4.98/4.59, N: 8.65/8.33, S:6.60/5.99; M. W: 492.03 g/mol.

7.2.4.5. (S)-3-((4-chlorobenzyl)thio)-4-(4-chlorophenyl)-5-(1-(6-methoxynaphtalen-2-yl)ethyl)-4H-1,2,4-triazole (5b). Yield: 20%, Mp: 114−116 °C, Rf x 100 (M1): 11, white solid. ^{1}H NMR: (300 MHz) (DMSO-d_6/TMS) δ ppm: 1.64 (d, J = 7.2 Hz, 3H, −CH−C<u>H</u>$_3$); 3.85 (s, 3H, O−CH$_3$); 4.11 (q, J = 6.6 Hz, J = 6.9 Hz, 1H, -C<u>H</u>-CH$_3$); 4.27 (s, 2H,

S−C<u>H</u>$_2$); 6.99−7.66 (m, 14H, Ar−<u>H</u>). ^{13}C NMR (125 MHz, DMSO-d_6) δ$_C$ ppm; 158.41 (C-6), 157.58 (C-18), 150.13 (C-14), 137.32 (C-33), 136.86 (C-28), 134.87 (C-22), 133.50 (C-9), 132.51 (C-27), 132.12 (C-2), 131.18 (C-23, C-24), 129.82 (C-3), 129.70 (C-1), 129.44 (C-7), 128.79 (C-10), 128.68 (C-25, C-26), 127.50 (C-30, C-29), 126.15 (C-31, C-32), 125.74 (C-8), 119.13 (C-5), 106.17 (C-4), 55.49 (C-12), 36.71 (C-13), 36.47 (C-21), 21.17 (C-19). FT-IR v$_{max}$ (cm^{-1}): 3033 (*C*−H), 1631, 1605 (C=N), 1260 (*C*−S). Anal. Calcd for C$_{28}$H$_{23}$Cl$_2$N$_3$OS·H$_2$O (calculated/found) C: 62.45/62.97, H: 4.68/4.30, N: 7.80/7.61, S:5.95/ 5.59; M. W: 538.49 g/mol.

7.2.4.6. (S)-3-((2,6-dichlorobenzyl)thio)-4-(4-chlorophenyl)-5-(1-(6-methoxynaphtalen-2-yl)ethyl)-4H-1,2,4-triazole (5c). Yield: 53.3%, Mp: 140−144 °C, Rf x 100 (M_2): 18, white solid. ^{1}H NMR: (300 MHz) (DMSO-d_6/TMS) δ ppm: 1.66 (d, J = 7.2 Hz, 3H, −CH−C<u>H</u>$_3$); 3.85 (s, 3H, O−CH$_3$); 4.15 (q, J = 6.9 Hz, J = 6.9 Hz, 1H, -C<u>H</u>-CH$_3$); 4.25−4.36 (dd, J = 12.9 Hz, J = 12.9 Hz, 2H, S−C<u>H</u>$_2$); 7.04−7.68 (m, 13H, Ar−<u>H</u>). ^{13}C NMR (125 MHz, DMSO-d_6) δ$_C$ ppm; 158.98 (C-6), 157.59 (C-18), 148.73 (C-14), 137.35 (C-33), 135.27 (C-28), 134.83 (C-22), 133.52 (C-9), 132.67 (C-23, C-24), 132.28 (C-2), 130.72 (C-25, C-26), 129.75 (C-3), 129.44 (C-1, C-7), 128.79 (C-10), 128.67 (C-27), 127.46 (C-30, C-29), 126.26 (C-31, C-32), 125.79 (C-8), 119.16 (C-5), 106.18(C-4), 55.60 (C-12), 36.85 (C-13), 34.44 (C-21), 21.25 (C-19). FT-IR v$_{max}$ (cm^{-1}): 3070 (*C*−H), 1625, 1601 (C=N), 1268 (*C*−S). Anal. Calcd for C$_{28}$H$_{22}$Cl$_3$N$_3$OS (calculated/found) C: 60.60/60.00, H: 4.00/3.94, N: 7.57/7.46, S: 5.78/5.68; M. W: 554.92 g/mol.

7.2.4.7. (S)-3-((4-fluorobenzyl)thio)-4-(4-chlorophenyl)-5-(1-(6-methoxynaphtalen-2-yl)ethyl)-4H-1,2,4-triazole (5d). Yield: 24%, Mp: 118−122 °C, Rf x 100 (M_2): 11, white solid. ^{1}H NMR: (300 MHz) (DMSO-d_6/TMS) δ ppm: 1.64 (d, J = 7.2 Hz, 3H, −CH−C<u>H</u>$_3$); 3.85 (s, 3H, O−CH$_3$); 4.12 (q, J = 7.2 Hz, J = 7.2 Hz, 1H, -C<u>H</u>-CH$_3$); 4.28 (s, 2H, S−C<u>H</u>$_2$); 6.99−7.66 (m, 14H, Ar−<u>H</u>). ^{13}C NMR (125 MHz, DMSO-d_6) δ$_C$ ppm; 158.36 (C-6), 157.57 (C-18), 150.25 (C-14), 137.34 (C-33), 134.87 (C-28), 133.92 (C-22), 133.90 (C-27), 133.49 (C-9), 132.15 (C-27), 131.41 (C-2), 131.35 (C-8), 129.85 (C-7), 129.70 (C-1), 129.44 (C-3), 128.68 (C-10), 127.47 (C-30, C-29), 126.17 (C-31, C-32), 125.72 (C-23, C-24), 119.12 (C-5), 115.71 (C-25), 115.54 (C-26), 106.15 (C-4), 55.59 (C-12), 36.68 (C-13), 36.39 (C-21), 21.21 (C-19). FT-IR v$_{max}$ (cm^{-1}): 3046 (*C*−H), 1631, 1604 (C=N), 1227 (*C*−S). Anal. Calcd for C$_{28}$H$_{22}$ClN$_3$OS. 3/2H$_2$O (calculated/found) C: 63.33/63.93, H: 4.94/ 4.23, N: 7.91/7.79, S: 6.04/5.59; M. W: 531.04 g/mol.

7.2.4.8. (S)-3-((4-methylbenzyl)thio)-4-(4-chlorophenyl)-5-(1-(6-methoxynaphtalen-2-yl)ethyl)-4H-1,2,4-triazole (5e). Yield: 33%, Mp: 79−81 °C, Rf x 100 (M_2): 14, white solid. ^{1}H NMR: (300 MHz) (DMSO-d_6/TMS) δ ppm: 1.65 (d, J = 7.2 Hz, 3H, −CH−C<u>H</u>$_3$); 2.15 (s, 3H, Ar−CH$_3$); 3.85 (s, 3H, O−CH$_3$); 4.05−4.12 (q, J = 6.9 Hz, J = 6.9 Hz, 1H, -C<u>H</u>-CH$_3$); 4.17−4.22 (dd, J = 12.9 Hz, J = 12.9 Hz, 2H, S−C<u>H</u>$_2$); 6.97−7.67 (m, 14H, Ar−<u>H</u>). ^{13}C NMR (125 MHz, DMSO-d_6) δ$_C$ ppm; 158.34 (C-6), 157.59 (C-18), 150.27 (C-14), 137.36 (C-33), 137.11 (C-28), 134.79 (C-22), 134.46 (C-27), 133.51 (C-8), 132.19 (C-2), 129.78 (C-3), 129.71 (C-1), 129.46 (C-7), 129.40 (C-10), 129.17 (C-25, C-26), 128.69 (C-30, C-29), 127.47 (C-23, C-24), 126.20 (C-31, C-32), 125.76 (C-9), 119.12 (C-5), 106.16 (C-4), 55.60 (C-12), 37.56 (C-13), 36.73 (C-21), 21.17 (C-19), 21.00 (C-35). FT-IR v$_{max}$ (cm^{-1}): 3054 (*C*−H), 1631, 1605 (C=N), 1263 (*C*−S). Anal. Calcd for C$_{29}$H$_{26}$ClN$_3$OS (calculated/found) C: 69.65/69.18, H: 5.24/4.87, N: 8.40/8.27, S: 6.41/5.98, M. W: 500.05 g/mol.

7.2.4.9. (S)-3-((4-chlorobenzyl)thio)-4-(4-fluorophenyl)-5-(1-(6-methoxynaphtalen-2-yl)ethyl)-4H-1,2,4-triazole (5f). Yield: 33%, Mp: 150−152 °C, Rf x 100 (M_2): 21, white solid. ^{1}H NMR: (300 MHz) (DMSO-d_6/TMS) δ ppm: 1.64 (d, J = 7.2 Hz, 3H, −CH−C<u>H</u>$_3$); 3.84 (s, 3H, -O-CH$_3$); 4.11 (q, J = 6.9 Hz, J = 6.9 Hz, 1H, -C<u>H</u>-CH$_3$); 4.28 (s, 2H,

-S-C$\underline{H}_2$-); 6.98–7.66 (m, 14H, Ar–H). ^{13}C NMR (125 MHz, DMSO-d_6) δ_C ppm; 163.60 (C-33), 161.63 (C-28), 158.54 (C-6), 157.56 (C-18), 150.32 (C-14), 137.38 (C-27), 136.89 (C-22), 133.49 (C-8), 132.48 (C-2),131.20 (C-9), 130.26 (C-23), 130.18 (C-24), 129.81 (C-3), 129.53 (C-1), 129.50 (C-7), 129.44 (C-30, C-29), 128.78 (C-10), 128.68 (C-25, C-26), 127.47 (C-1), 126.16 (C-31, C-32), 125.70 (C-9), 119.13 (C-5), 106.16 (C-4), 55.59 (C-12), 36.72 (C-13), 36.32 (C-21), 21.16 (C-19). FT-IR v_{max} (cm^{-1}): 3061 (C–H), 1628, 1605 (C=N), 1227 (C–S). Anal. Calcd for C$_{28}$H$_{23}$ClFN$_3$OS·3/2H$_2$O (calculated/found) C: 63.33/62.47, H: 4.93/4.22, N: 7.91/7.78, S: 6.04/5.87. M. W: 531.04 g/mol.

7.2.4.10. (S)-3-((2,6-dichlorobenzyl)thio)-4-(4-fluorophenyl)-5-(1-(6-methoxynaphtalen-2-yl)ethyl)-4H-1,2,4-triazole (5g). Yield: 26%, Mp: 80 °C, Rf x 100 (M$_2$): 26, white solid. ^{1}H NMR (300 MHz) (DMSO-d_6/TMS) δ ppm: 1.67 (d, J = 12.9 Hz, 3H, –CH–C$\underline{H}_3$); 3.85 (s, 3H, -O-CH$_3$); 4.12 (m, 1H, -C$\underline{H}$-CH$_3$); 4.27–4.38 (dd, J = 12.9 Hz, J = 12.9 Hz, 2H, -S-C$\underline{H}_2$-); 7.03–7.67 (m, 13H, Ar–H). ^{13}C NMR (125 MHz, DMSO-d_6) δ_C ppm; 163.59 (C-33), 161.62 (C-28), 159.10 (C-6), 157.58 (C-18), 148.93 (C-14), 137.41 (C-23, C-24), 135.27 (C-22), 133.52 (C-9), 132.69 (C-23, C-24), 130.71(C-2), 130.29 (C-3), 130.22 (C-25),129.69 (C-26) 129.67 (C-3), 129.44 (C-1, C-7), 129.10 (C-10), 128.67 (C-27), 127.44 (C-30, C-29), 126.27 (C-31, C-32), 125.76 (C-8), 119.15 (C-5), 106.18 (C-4), 55.59 (C-12), 36.88 (C-13), 34.38 (C-21), 21.23 (C-19). FT-IR v_{max} (cm^{-1}): 3061 (C–H), 1633, 1605 (C=N), 1229 (C–S). Anal. Calcd for C$_{28}$H$_{22}$Cl$_2$FN$_3$OS·H$_2$O (calculated/found) C: 60.43/60.50, H: 4.35/4.06, N: 7.55/7.27, S: 5.76/5.83. M. W: 556.48 g/mol.

7.2.4.11. (S)-3-((4-fluorobenzyl)thio)-4-(4-fluorophenyl)-5-(1-(6-methoxynaphtalen-2-yl)ethyl)-4H-1,2,4-triazole (5h). Yield: 26%, Mp: 121 °C, Rf x 100 (M$_2$): 23, white solid. ^{1}H NMR (300 MHz) (DMSO-d_6/TMS) δ ppm: 1.64 (d, J = 7.2 Hz, 3H, –CH–C$\underline{H}_3$); 3.84 (s, 3H, -O-CH$_3$); 4.07–4.14 (q, J = 6.9 Hz, J = 6.9 Hz 1H, -C$\underline{H}$-CH$_3$); 4.28 (s, 2H, -S-C$\underline{H}_2$-); 6.99–7.65 (m, 14H, Ar–H). FT-IR v_{max} (cm^{-1}): 3067 (C–H), 1631, 1607 (C=N), 1264 (C–S). Anal. Calcd for C$_{28}$H$_{23}$F$_2$N$_3$OS·H$_2$O (calculated/found) C: 66.52/66.70, H: 4.98/4.56, N: 8.31/8.22, S: 6.34/6.45. M. W: 505.58 g/mol.

7.2.4.12. (S)-3-((4-methylbenzyl)thio)-4-(4-fluorophenyl)-5-(1-(6-methoxynaphtalen-2-yl)ethyl)-4H-1,2,4-triazole (5i). Yield: 33%, Mp: 163–165 °C, Rf x 100 (M$_2$): 27, white solid. ^{1}H NMR (300 MHz) (DMSO-d_6/TMS) δ ppm: 1.65 (d, J = 7.2 Hz, 3H, –CH–C$\underline{H}_3$); 2.16 (s, 3H, Ar-CH$_3$); 3.85 (s, 3H, -O-CH$_3$); 4.04–4.11 (q, J = 6.9 Hz, J = 7.2 Hz 1H, -C$\underline{H}$-CH$_3$); 4.16–4.25 (t, 2H, -S-CH$_2$-); 6.98–7.66 (m, 14H, Ar–H). FT-IR v_{max} (cm^{-1}): 3061 (C–H), 1633, 1606 (C=N), 1222 (C–S). Anal. Calcd for C$_{29}$H$_{26}$FN$_3$OS (calculated/found) C: 72.02/71.93, H: 5.42/5.33, N: 8.69/8.65, S: 6.63/6.82. M. W: 483.61 g/mol.

7.2.4.13. (S)-3-((3-methoxybenzyl)thio)-4-(4-chlorophenyl)-5-(1-(6-methoxynaphtalen-2-yl)ethyl)-4H-1,2,4-triazole (5j). Yield: 47%, Mp: 116 °C, Rf x 100 (M$_2$): 24, white solid. ^{1}H NMR (300 MHz) (DMSO-d_6/TMS) δ ppm: 1.64 (d, J = 6.9 Hz, 3H, –CH–C$\underline{H}_3$); 3.67 (s, 3H, Ar-O-CH$_3$); 3.85 (s, 3H, -O-CH$_3$); 4.08–4.15 (q, J = 6.9 Hz, J = 6.9 Hz, 1H, -C$\underline{H}$-CH$_3$); 4.24 (s, 2H, -S-CH$_2$-); 6.77–7.66 (m, 14H, Ar–H). FT-IR v_{max} (cm^{-1}): 3091 (C–H), 1635, 1601 (C=N), 1268 (C–S). Anal. Calcd for C$_{29}$H$_{26}$ClN$_3$O$_2$S (calculated/found) C: 67.49/67.17, H: 5.08/4.98, N: 8.14/8.16, S: 6.21/6.32. M. W: 516.05 g/mol.

7.2.4.14. (S)-3-((4-methoxybenzyl)thio)-4-(4-chlorophenyl)-5-(1-(6-methoxynaphtalen-2-yl)ethyl)-4H-1,2,4-triazole (5k). Yield: 59%, Mp: 122.3 °C, Rf x 100 (M$_2$): 19, white solid. ^{1}H NMR (300 MHz) (DMSO-d_6/TMS) δ ppm: 1.64 (d, J = 7.2 Hz, 3H, –CH–C$\underline{H}_3$); 3.60 (s, 3H, Ar-OC$\underline{H}_3$); 3.85 (s, 3H, -O-CH$_3$); 4.10 (q, J = 6.9 Hz, J = 6.9 Hz, 1H, -CH-CH$_3$); 4.22 (s, 2H, -S-C$\underline{H}_2$-); 6.74–7.66 (m, 14H, Ar–H). FT-IR v_{max} (cm^{-1}): 3091 (C–H), 1607 (C=N), 1239 (C–S). Anal. Calcd for

C$_{29}$H$_{26}$ClN$_3$O$_2$S 0.3/2H$_2$O (calculated/found) C: 64.14/63.82, H: 5.38/4.96, N: 7.74/7.34, S: 5.90/5.81. M. W: 543.07 g/mol.

7.2.4.15. (S)-3-((3-methoxybenzyl)thio)-4-(4-fluorophenyl)-5-(1-(6-methoxynaphtalen-2-yl)ethyl)-4H-1,2,4-triazole (5l). Yield: 30%, Mp: 99.7 °C, Rf x 100 (M$_2$): 29, white solid. ^{1}H NMR: (300 MHz) (DMSO-d_6/TMS) δ ppm: 1.64 (d, J = 7.2 Hz, 3H, –CH–C$\underline{H}_3$); 3.60 (s, 3H, Ar-O-C$\underline{H}_3$); 3.86 (s, 3H, -O-CH$_3$); 4.10 (q, J = 6.9 Hz, J = 6.9 Hz, 1H, -C$\underline{H}$-CH$_3$); 4.24 (s, 2H, -S-C$\underline{H}_2$-); 6.77–7.79 (m, 14H, Ar–H). FT-IR v_{max} (cm^{-1}): 3064 (C–H), 1634, 1600 (C=N), 1264 (C–S). Anal. Calcd for C$_{29}$H$_{26}$FN$_3$O$_2$S·2H$_2$O (calculated/found) C: 65.03/65.54, H: 5.65/5.04, N: 7.84/8.09. M. W: 535.63 g/mol.

7.2.4.16. (S)-3-((4-methoxybenzyl)thio)-4-(4-fluorophenyl)-5-(1-(6-methoxynaphtalen-2-yl)ethyl)-4H-1,2,4-triazole (5m). Yield: 35%, Mp: 125.3 °C, Rf x 100 (M$_2$): 20, white solid. ^{1}H NMR (300 MHz) (DMSO-d_6/TMS) δ ppm: 1.64 (d, J = 6.9 Hz, 3H, –CH–C$\underline{H}_3$); 3.64 (s, 3H, Ar-O-CH$_3$); 3.85 (s, 3H, -O-CH$_3$); 4.10 (q, J = 6.9 Hz, J = 6.9 Hz, 1H, -C$\underline{H}$-CH$_3$); 4.22 (s, 2H, -S-C$\underline{H}_2$-); 6.76–7.66 (m, 14H, Ar–H). FT-IR v_{max} (cm^{-1}): 3562, 3412 (O–H from water); 3063 (C–H), 1631, 1605 (C=N), 1264 (C–S). Anal. Calcd for C$_{29}$H$_{26}$FN$_3$O$_2$S·2H$_2$O (calculated/found) C: 65.03/64.49, H: 5.65/5.30, N: 7.84/7.61, S: 5.99/5.68. M. W: 535.63 g/mol.

7.2.4.17. (S)-3-((2,4,6-trimethylphenyl)thio)-4-(4-fluorophenyl)-5-(1-(6-methoxynaphtalen-2-yl)ethyl)-4H-1,2,4-triazole (5n). Yield: 41%, Mp: 143,6 °C, Rf x 100 (M$_2$): 18, white solid. ^{1}H NMR: (300 MHz) (DMSO-d_6/TMS) δ ppm: 1.66 (d, J = 6.9 Hz, 3H, –CH–C$\underline{H}_3$); 2.08 (s, 9H, Ar-CH$_3$); 3.85 (s, 3H, O–CH$_3$); 4.06–4.28 (m, 1H, -C$\underline{H}$-CH$_3$ and 2H, S–C$\underline{H}_2$); 6.69–7.67 (m, 12H, Ar–$\underline{H}$). ^{13}C NMR (75 MHz, DMSO-d_6) δ_C ppm; 163.76 (C-33), 160.48 (C-6), 158.29 (C-28), 157.09 (C-18), 149.78 (C-14), 136.88 (C-23, C-24), 136.81 (C-27), 136.59 (C-22), 133.09 (C-9), 129.99 (C-2), 129.87 (C-3), 129.21 (C-25), 129.69 (C-26) 129.18 (C-7), 129.00 (C-1), 128.92 (C-10), 128.75 (C-22), 128.19 (C-30, C-29), 126.98 (C-31), 125.74 (C-32), 116.19 (C-8), 118.64 (C-5), 105.65 (C-4), 55.10 (C-12), 36.33 (C-21), 34.38 (C-13), 20.61 (C-19), 20.32(C-37), 18.83 (C-35, C-36). FT-IR v_{max} (cm^{-1}) = 3062 (C–H); 1631, 1604 (C=N), 1264 (C–S). Anal. Calcd for C$_{31}$H$_{30}$FN$_3$OS·1/3H$_2$O (calculated/found) C: 71.93/71.28, H: 5.97/5.82, N: 8.12/8.02, S: 6.19/5.64. M. W: 517.68 g/mol. HR-MS (ESI) *m/z*: Calculated for [C$_{31}$H$_{30}$FN$_3$NaOS$^+$] 534.1986, found 534.1990.

7.2.4.18. (S)-3-((2,6-dichlorobenzyl)thio)-4-(3-chlorophenyl)-5-(1-(6-methoxynaphtalen-2-yl)ethyl)-4H-1,2,4-triazole (5o). Yield: 40%, Mp: 114.6 °C, Rf x 100 (M$_2$): 42, white solid. ^{1}H NMR (300 MHz) (DMSO-d_6/TMS) δ ppm: 1.67 (d, J = 6.9 Hz, 3H, –CH–C$\underline{H}_3$); 3.85 (s, 3H, -O-C$\underline{H}_3$); 4.11–4.18 (q, J = 6.9 Hz, J = 6.3 Hz, 1H, -C$\underline{H}$-CH$_3$); 4.24–4.37 (q, J = 12.9 Hz, J = 12,9 Hz, 2H, -S-C$\underline{H}_2$-); 7.03–7.68 (m, 12H, Ar–H). FT-IR v_{max} (cm^{-1}): 3056 (C–H), 1631, 1604 (C=N), 1278 (C–S). Anal. Calcd for C$_{28}$H$_{22}$Cl$_3$N$_3$OS (calculated/found) C: 60.60/60.36, H: 4.00/3.93, N: 7.57/7.18, S: 5.78/5.32. M. W: 554.92 g/mol.

7.2.4.19. (S)-3-((2,4,6-trimethylbenzyl)thio)-4-(3-chlorophenyl)-5-(1-(6-methoxynaphtalen-2-yl)ethyl)-4H-1,2,4-triazole (5p). Yield: 51%, Mp: 173.4 °C, Rf x 100 (M$_2$): 45, white solid. ^{1}H NMR: (300 MHz) (DMSO-d_6/TMS) δ ppm: 1.65–1.66 (d, J: 7.2 Hz, 3H, –CH–C$\underline{H}_3$); 2.02 (s, 9H, Ar-CH$_3$); 3.85 (s, 3H, -O-CH$_3$); 4.04–4.28 (q, 1H, -C$\underline{H}$-CH$_3$ ve 2H, -S-C$\underline{H}_2$-); 6.62–7.69 (m, 12H, Ar–H). FT-IR v_{max} (cm^{-1}): 3089 (C–H), 1633, 1604 (C=N), 1216 (C–S). Anal. Calcd for C$_{31}$H$_{30}$ClN$_3$OS (calculated/found) C: 70.50/70.61, H: 5.73/5.62, N: 7.96/7.74, S: 6.07/5.92. M. W: 528.11 g/mol.

7.3. Molecular docking and dynamics simulation

The molecular docking study of all synthesized compounds was

studied in the Faculty of Engineering and Natural Sciences, Department of Bioinformatics and Genetic, Kadir Has University. The X-ray crystal structure of human methionine aminopeptidase (type II) in complex with spiroepoxytriazole inhibitor (+)-31a (PDB ID: 5CLS; resolution 1.75 Å) was downloaded from the protein data bank (PDB) (https://www.rcsb.org). The inhibitor, water molecules and non-interacting ions were removed; and hydrogens were added based on the protonation state of the titratable residues at pH 7.4. The geometry of the protein was then cleaned using "Clean Geometry" toolkit; and fully prepared using "Prepare Protein" toolkit of Biovia Discovery Studio 4.5 software. The three-dimensional (3D) structures of the compounds were drawn, their geometry was optimized and prepared using "Prepare Small Molecules" toolkit of Biovia Discovery Studio 4.5. The docking files were prepared using AutodockTools (ADT) in which Gasteiger partial charges were added to each atom. Grid box of dimension 60, 60, 60 Å was centered near cobalt (Co^{2+}) ion, covering the entire active site. Docking was performed using Autodock 4.2 Lamarckian Genetic Algorithm (GA) (http://autodock.scripps.edu) in which 20 GA runs were performed with 10 million energy evaluation for each compound [34]. The protein-ligand interactions were visualized, both 3D and 2D interaction diagrams were generated using Biovia Discovery Studio (DS) 4.5 program [35].

To relax the complex structure and examine the stability of ligand binding mode, the free form of MetAP2 and its complex with Compound **5n** were submitted to MD simulation using Nanoscale MD (NAMD) software (http://www.ks.uiuc.edu/Research/namd/) [36]. The input files were generated using CHARMM-GUI server (http://www.charmm.org) [37] where Na^+ ion was added to the ionic concentration of 0.15 M. The CHARMM General Force Field (CGenFF) server was used to parameterize Compound **5n** (https://cgenff.paramchem.org/) [38]. The two systems were minimization by steepest descent method for 10,000 steps; equilibrated for 5 ns in standard number of particle, volume, and temperature (NVT) ensemble; and finally submitted to unrestrained 100 ns-production runs in standard number of particle, pressure, and temperature (NPT) ensemble. A timestep of 2fs was used, and trajectory frame was collected at the interval of every 10 ps. Both trajectories were clustered using RMSD cutoff of 2.5 Å and the representative of the most abundant cluster (78% for the free MetAP2 system, and 89% for the MetAP2-Compund **5n** complex) were analyzed using Biovia DS 4.5 program [35].

7.4. Anticancer activity

The anticancer activity of all synthesized compounds was evaluated by using MTS [28] and Western blot methods in the Faculty of Pharmacy, Erciyes University. The anticancer activity of the all synthesized compounds was evaluated against PC-3, DU-145 and LNCaP. Cell proliferative activity was measured using the 3-(4,5-dimethylthiazol-2-yl)-5-(3-carboxymethoxyphenyl)-2-(4-sulfophenyl)-2*H*-tetrazolium (MTS) assay kit (Promega, Madison, WI, USA). Cisplatin was used as the positive sensitivity reference standard for cell lines.

7.4.1. Western blot method

1×10^6 cells (n = 3) were inoculated in RPMI-1640 without phenol red containing 1% FBS in each well of a 6-well cell culture dish and were allowed to sit for 24 h at the bottom of the culture dish. Compound **5n** were then applied to the cells at varying concentrations for 0, 15, 60, 120 min. At the end of the period, the medium was discarded, and the cells were homogenized with lysis solution. Total protein was determined in the homogenates. Protein samples were analyzed by the conventional Western blot method [39].

7.5. Methionine aminopeptidase assay

The enzyme assay was adopted from Li et al. with several modifications. Methionine aminopeptidase activity was determined spectrophotometrically in a 96-well microtitre plates using a Microplate Reader (Model 680XR, Bio-Rad, USA). The reaction mixture contained 100 μl of 2.5 mmol/l L-methionine p-nitroanilide (l-Met-pNA in %10 DMSO/H_2O), 100 μl of Assay buffer 50 mM MOPS, 10 mM NaCl, 100 μM $CoCl_2$ pH 7.2), and 50 μl enzyme sample (50 μg/6250 μL), making the total reaction volume to 250 μl. The reaction mixture was mixed well and incubated at 37 °C for 30 min. The reaction was stopped by addition of 100-μl glacial acetic acid and the absorbance was measured at 405 nm [40].

7.6. In vivo studies

7.6.1. Development of prostate cancer animal models and investigation of compound 5n (SGK 636) treatment potential

$5 \times 10^6 - 6 \times 10^6$ cell/100 μL LNCaP prostate cancer cells were injected subcutaneously into male nude mice. Cancerous tissues were visualized by using in vivo Imaging System (IVIS Spectrum-Perkin-Elmer) at Ege University, Center for Drug Research & Development and Pharmacokinetic Applications (ARGEFAR). The experimental protocol was approved by the Local Animal Ethical Committee of Ege University (Approval No. E.U.2016−092). 10 nmol/100 μL Xenolight RediJect 2-DG-750 Probe was administered by intravenous (iv) tail vein after anesthetizing the mice with isoflurane. The settings of the IVIS spectrum instrument were adjusted to be Binning = 8, f/stop = 2, Excitation = 745 nm and Emission = 820 nm throughout the experiment.

- Group 1: Nude mouse which have Xenograft prostate cancer model constructed with LNCaP cell lines no treatment with **SGK 636** for 15 days (n = 6).
- Group 2: Nude mouse which have Xenograft prostate cancer model constructed with LNCaP cell lines treated with compound **5n** (**SGK 636**) for 15 days (n = 6). Treatment dose (0.27 mg all synthesized compound **5n** (**SGK 636**)/100 μL of saline solution was injected intraperitoneal every 4 days.).

7.6.2. Blood analysis of treated prostate cancer animals

The blood parameters Albumin (ALB), Alkaline Phosphatase (ALP), Alanine Transaminase (ALT), Total Bilirubin (TBIL), Blood Urea Nitrogen (BUN), Phosphate (PHOS), Keratin (CRE), Glucose (GLU), Sodium (Na), Potassium (K), Total Protein (TP), and globulin (GLOB) were analyzed by using VETSCAN automatic biochemical blood analyser, after 3 doses of treatment.

Accession codes

The molecular modeling is using 5CLS on RCSB Protein Data Bank (www.rscb.org).

Author contributions

The manuscript was written through contributions of all authors. All authors have given approval to the final version of the manuscript. ‡These authors contributed equally. (Concept −Ş.G.K, H.Y.K.; Design − Ş.G.K, H.Y.K, K.B.; Supervision − Ş.G.K, H.Y.K,.; Resource − Ş.G.K, H.Y.K,.; Materials − Ş.G.K, H.Y.K, K.B, Y.Y, E.K, H.B, A.C, A.İ.U, K.Y.; Data collection and/or processing − Ş.G.K, H.Y.K, K.B, Y.Y, E.K, H.B, A.C, A.İ.U, K.Y.; Analysis and/or Interpretation − Ş.G.K, H.Y.K, K.B, Y.Y, E.K, H.B, A.C, A.İ.U, K.Y.; Literature Search − Ş.G.K, H.Y.K, K.B, Y.Y, E.K, H.B, A.C, A.İ.U, K.Y.; Writing − Ş.G.K, H.Y.K.;

Critical Reviews — Ş.G.K, H.Y.K, K.B, Y.Y, E.K, H.B, A.C, A.İ.U, K.Y).

Declaration of competing interest

Acknowledgements

Abbreviations

FT-IR	Fourier transform infrared
HR-MS	high resolution mass spectrometry
MetAP	methionine amino peptidase
MAPK	mitogen-activated protein kinase
MTT	(3-(4,5-dimethyl thiazol-2-yl)-2,5-diphenyltetrazolium bromide) colorimetric method
NMR	nuclear magnetic resonance
PC-3	DU-145
LNCaP	Human prostate cancer cell lines
IC_{50}	50% Inhibition Concentration
PCa	prostate cancer
TLC	thin layer chromatography
ALB	albumin
ALP	alkaline phosphatase
ALT	alanine transaminase
TBIL	total bilirubin
BUN	blood urea nitrogen
PHOS	phosphate
CRE	keratin
GLU	glucose
Na	sodium
K	potassium
TP	total protein
GLOB	globulin

Appendix A. Supplementary data

Supporting Information. Experimental data (^{1}H NMR, FT-IR, elemental analysis results and HR-Mass) of novel thio-semicarbazides **3a, 3d**, 1,2,4-triazole-3-thione **4a**, thioether **5a-p** molecules.

Supplementary data to this article can be found online at https://doi.org/10.1016/j.ejmech.2020.112841.

References

[1] T. Garrabrant, R.T. Tuman, D. Ludovici, R. Tominovich, R.L. Simoneaux, R.A. Galemmo Jr., D.L. Johnson, Small molecule inhibitors of methionine aminopeptidase type 2 (MetAP-2) fail to inhibit endothelial cell proliferation or formation of microvessels from rat aortic rings in vitro, Angiogenesis 7 (2004) 91−96, https://doi.org/10.1007/s10456-004-6089-7.

[2] M.İ. Han, H. Bekçi, A. Cumaoğlu, Ş.G. Küçükgüzel, Synthesis and character-ization of 1,2,4-triazole containing hydrazide-hydrazones derived from (S)-Naproxen as anticancer agents, Marmara Pharm. J. 22 (4) (2015) 559−569, https://doi.org/10.12991/jrp.2018.98.

[3] M.İ. Han, H. Bekçi, A.İ. Uba, Y. Yıldırım, E. Karasulu, A. Cumaoğlu, H.Y. Karasulu, K. Yelekçi, Ö. Yılmaz, Ş.G. Küçükgüzel, Synthesis, molecular modeling, in vivo study, and anticancer activity of 1,2,4-triazole containing hydrazide-hydrazones derived from (S)-naproxen, Arch. Pharm. Chem. Life. Sci. (2019), e1800365, https://doi.org/10.1002/ardp.201800365.

[4] Ö. Yılmaz, B. Bayer, H. Bekçi, A.İ. Uba, A. Cumaoğlu, K. Yelekçi, Ş.G. Küçükgüzel, Synthesis, anticancer activity on prostate cancer cell lines and molecular modeling studies of flurbiprofen-thioether derivatives as potential target of MetAP (type II), Med. Chem. 16 (6) (2020) 734−749, https://doi.org/10.2174/1573406415666190613162322.

[5] P. Selvakumar, A. Lakshmikuttyamma, R. Kanthan, S.C. Kanthan, J.R. Dimmock, R.K. Sharma, High expression of methionine aminopeptidase 2 in human colorectal adenocarcinomas, Clin. Canc. Res. 10 (2004) 2771−2775, https://doi.org/10.1158/1078-0432.CCR-03-0218.

[6] P. Selvakumar, A. Lakshmikuttyamma, J.R. Dimmock, R.K. Sharma, Methionine aminopeptidase 2 and cancer, Biochim. Biophys. Acta 1765 (2006) 148−154, https://doi.org/10.1016/j.bbcan.2005.11.001.

[7] P. Selvakumar, A. Lakshmikuttyamma, U. Das, H.N. Pati, J.R. Dimmock, R.K. Sharma, NC2213: a novel methionine aminopeptidase 2 inhibitor in hu-man colon cancer HT29 cells, Mol. Canc. 8 (2009) 65, https://doi.org/10.1186/1476-4598-8-65.

[8] Y.-P. Huo, J. Sun, Z.-H. Pang, P.-C. Lv, D.-D. Li, L. Yan, H.-J. Zhang, E.X. Zheng, J. Zhao, H.-L. Zhu, Synthesis and antitumor activity of 1,2,4-triazoles having 1,4-benzodioxan fragment as a novel class of potent methionine amino-peptidase type II inhibitors, Bioorg. Med. Chem. 19 (2011) 5948−5954, https://doi.org/10.1016/j.bmc.2011.08.063.

[9] I. Çoruh, Ö. Çevik, K. Yelekçi, T. Djikic, Ş.G. Küçükgüzel, Synthesis, anticancer activity and molecular modeling of etodolac-thioether derivatives as potent methionine aminopeptidase (type II) inhibitors, Arch Pharm Chem Life Sci e351 (2018), e1700195, https://doi.org/10.1002/ardp.201700195.

[10] J. Xie, M. Rice, Y. Cheng, G. Song, C. Kunder, J.D. Brooks, T. Stoyanova, J. Rao, Methionine aminopeptidase II (MetAP2) activated in situ self-assembly of small-molecule probes for imaging prostate cancer, in: Proceedings of the AACR Special Conference: Prostate Cancer: Advances in Basic, Translational, and Clinical Research; 2017 Dec 2-5 78, AACR; Cancer Res, Orlando, Florida. Philadelphia (PA), 2018, https://doi.org/10.1158/1538-7445.PRCA2017-B068 (16 Suppl):Abstract nr B068.

[11] S.Q. Yin, J.J. Wang, C.M. Zhang, Z.P. Liu, The development of MetAP-2 in-hibitors in cancer treatment, Curr. Med. Chem. 19 (7) (2012) 1021−1035, https://doi.org/10.2174/092986712799320709.

[12] C.J. Logothethis, K.K. Wu, L.D. Finn, D. Daliani, W. Figg, H. Ghaddar, J.U. Gutterman, Phase I trial of the angiogenesis inhibitor TNP-470 for pro-gressive androgen-independent prostate cancer, Clin. Canc. Res. 7 (5) (2001) 1198−1203.

[13] L. Türkeri, Kronik prostatit, enflamasyon ve prostat kanseri, Üroonkoloji Bülteni 3 (2007) 11−15.

[14] M.I. Han, Ş.G. Küçükgüzel, Anticancer and antimicrobial activities of naproxen and naproxen derivatives, Mini Rev. Med. Chem. 20 (13) (2020) 1300−1310, https://doi.org/10.2174/1389557520666200505124922.

[15] S. Srinivas, D. Feldman, A phase II trial of calcitriol and naproxen in recurrent prostate cancer, Anticancer Res. 29 (2009) 3605−3610. PMID: 19667155.

[16] R.A. Lubet, V.E. Steele, M.M. Juliana, C.J. Grubbs, Screening agents for pre-ventive efficacy in a bladder cancer model: study, design, end points and gefitinib and naproxen efficacy, J. Urol. 183 (4) (2010) 1598−1603, https://doi.org/10.1016/j.juro.2009.12.001.

[17] M.-S. Kim, J.-E. Kim, D.Y. Lim, Z. Huang, H. Chen, A. Langfald, R.A. Lubet, C.J. Grubbs, Z. Dong, A.M. Bode, Naproxen induces cell cycle arrest and apoptosis in human urinary bladder cancer cell lines and chemically induced cancers by targeting PI3-K, Canc. Prev. Res. 7 (2) (2014) 236−245, https://doi.org/10.1158/1940-6207.CAPR-13-0288.

[18] Z. Culig, M. Puhr, Interleukin-6 and prostate cancer: current developments and unsolved questions, Mol. Cell. Endocrinol. 462 (2018) 25−30, https://doi.org/10.1016/j.mce.2017.03.012.

[19] P. Çıkla, D. Özsavcı, Ö. Bingöl-Özakpınar, A. Şener, Ö. Çevik, S. Özbaş-Turan, J. Akbuğa, F. Şahin, Ş.G. Küçükgüzel, Synthesis, cytotoxicity, and pro-apoptosis activity of etodolac hydrazide derivatives as anticancer agents, Arch. Pharm. Chem. Life. Sci. 346 (2013) 367−379, https://doi.org/10.1002/ardp.201200449.

[20] Ş.G. Küçükgüzel, P. Çıkla-Süzgün, Recent advances bioactive 1,2,4-triazole-3-thiones, Eur. J. Med. Chem. 97 (2015) 830−870, https://doi.org/10.1016/j.ejmech.2014.11.033.

[21] G.P. Coşkun, T. Djikic, T.B. Hayal, N. Türkel, K. Yelekçi, F. Şahin, Ş.G. Küçükgüzel, Synthesis, molecular, docking and anticancer activity of diflunisal derivatives as cyclooxygenase enzyme inhibitor, Molecules 23 (8) (2018), https://doi.org/10.3390/molecules23081969, 1969.

[22] Y. Dadaş, G.P. Coşkun, Ö. Bingöl-Özakpınar, D. Özsavcı, Ş.G. Küçükgüzel, Synthesis and anticancer activity of some novel tolmetin thiosemicarbazides, Marmara Pharm. J. 19 (2015) 259−267, https://doi.org/10.12991/mpj.201519328306.

[23] Ş.G. Küçükgüzel, G.P. Coşkun, Macromolecular drug targets in cancer treat-ment and thiosemicarbazides as anticancer agents, Anticancer Agents Med

Chem 16 (10) (2016) 1288−1300, https://doi.org/10.2174/1871520616666160219160256.

[24] P.J. Harrington, E. Lodewijk, Twenty years of naproxen technology, Org. Process Res. Dev. 1 (1997) 72−76, https://doi.org/10.1021/op960009e.

[25] European Pharmacopoeia 7.0, Monographs N-O, p.2554-2555 (07/2008:0731).

[26] M. Amir, H. Kumar, S.A. Javed, Non-carboxylic analouges of naproxen: design, synthesis and pharmacological evaluation of some 1,3,4-oxadiazole/thiadiazole and 1,2,4-triazole derivatives, Arch. Pharmazie 340 (11) (2007) 577−585, https://doi.org/10.1002/ardp.200700065.

[27] J. Weako, A.I. Uba, Ö. Keskin, A. Gürsoy, K. Yelekçi, Identification of potential inhibitors of human methionine aminopeptidase (type II) for cancer therapy: structure-based virtual screening, ADMET prediction and molecular dynamics studies, Comput. Biol. Chem. 86 (2020) 107244, https://doi.org/10.1016/j.compbiolchem.2020.107244.

[28] N. Moğulkoç, Akciğer kanserlerinin semptomları, bulguları, in: A. Haydaroğlu (Ed.), Akciğer Kanserleri: Tanı Ve Tedavi, Ege Üniversitesi Basımevi, 2000, pp. 57−76.

[29] F.U. Kantar, Karaciğer fonksiyon testi yüksekliğine yaklaşım, Klinik Tıp Bilimleri Dergisi 5 (2) (2017) 30−38.

[30] S.A. Akuyam, O.K. Uchenna, A. Adamu, I.S. Aliyu, A. Mai, D.A. Dawotola, S.A. Adewuyi, Liver function tests profile in cancer patients on cytotoxic chemotherapy: a preliminary report, Niger. Postgrad. Med. J. 18 (1) (2011) 34−38.

[31] Suganya, R.S. Priya, T.R. Samuel, B. Rajagopalan, A study to evaluate the role of Bun/Creatinine ratio as a discriminator factor in azotemia, Int. J. Pharmaceut. Sci. Rev. Res. 40 (1) (2016) 131−134.

[32] J.H. Salazar, Overview of urea and creatinine, Lab. Med. 45 (1) (2014) E19−E20, https://doi.org/10.1309/LM920SBNZPJRJGUT.

[33] G. Cui, T. Zhang, F. Ren, W.-M. Feng, Y. Yao, J. Cui, G.-L. Zhu, Q.-L. Shi, High blood glucose levels correlate with tumor malignancy in colorectal cancer patients, Med. Sci. Mon. Int. Med. J. Exp. Clin. Res. 21 (2015) 3825−3833, https://doi.org/10.12659/MSM.894783.

[34] G. Morris, R. Huey, AutoDock4 and AutoDockTools4: automated docking with selective receptor flexibility, J. Comput. Chem. 30 (2009) 2785−2791, https://doi.org/10.1002/jcc.21256.

[35] Dassault Systemes BIOVIA, BIOVIA Discovery Studio 2017 R2: A Comprehensive Predictive Science Application for the Life Sciences, 2017. San Diego, CA, USA.

[36] J.C. Phillips, R. Braun, W. Wang, J. Gumbart, E. Tajkhorshid, E. Villa, C. Chipot, R.R.D. Skeel, L. Kale, K. Schulten, Scalable molecular dynamics with NAMD, J. Comput. Chem. 26 (2005) 1781−1802, https://doi.org/10.1002/jcc.20289.

[37] J. Lee, X. Cheng, J.M. Swails, M.S. Yeom, P.K. Eastman, J.A. Lemkul, S. Wei, J. Buckner, J.C. Jeong, Y. Qi, S. Jo, V.S. Pande, D.A. Case, C.L. Brooks, A.D. MacKerell, J.B. Klauda, W. Im, CHARMM-GUI input generator for NAMD, GROMACS, AMBER OpenMM and CHARMM/OpenMM simulations using the CHARMM36 additive force field, J. Chem. Theor. Comput. 12 (2016) 405−413, https://doi.org/10.1021/acs.jctc.5b00935.

[38] S. Kim, J. Lee, S. Jo, C.L. Brooks 3rd, H.S. Lee, W. Im, CHARMM-GUI ligand reader and modeler for CHARMM force field generation of small molecules, J. Comput. Chem. 38 (2017) 1879−1886, https://doi.org/10.1002/jcc.24829.

[39] A. Cumaoğlu, S. Dayan, A.O. Agkaya, Z. Ozkul, Z.N. Kalaycioglu Ozpozan, Synthesis and pro-apoptotic effects of new sulfonamide derivatives via activating p38/ERK phosphorylation in cancer cells, J. Enzym. Inhib. Med. Chem. 30 (3) (2015) 413−419, https://doi.org/10.3109/14756366.2014.940938.

[40] J.Y. Li, L.L. Chen, Y.M. Cui, Q.L. Luo, J. Li, F.J. Nan, Q.Z. Ye, Specificity for inhibitors of metal-substituted methionine aminopeptidase, Biochem. Biophys. Res. Commun. 307 (1) (2003) 172−179, https://doi.org/10.1016/s0006-291x(03)01144-6, 18.